



Published in final edited form as:

Dev Dyn. 2020 October ; 249(10): 1217–1242. doi:10.1002/dvdy.211.

Analysis of FGF20-regulated genes in organ of Corti progenitors by translating ribosome affinity purification

Lu M. Yang¹, Lisa Stout², Michael Rauchman², David M. Ornitz^{1,*}

¹Department of Developmental Biology, Washington University School of Medicine; St. Louis, Missouri, 63110; USA

²Division of Nephrology, Department of Medicine, Washington University School of Medicine; St. Louis, Missouri, 63110; USA

Abstract

Background: Understanding the mechanisms that regulate hair cell (HC) differentiation in the organ of Corti (OC) is essential to designing genetic therapies for hearing loss due to HC loss or damage. We have previously identified Fibroblast Growth Factor 20 (FGF20) as having a key role in HC and supporting cell differentiation in the mouse OC. To investigate the genetic landscape regulated by FGF20 signaling in OC progenitors, we employ Translating Ribosome Affinity Purification combined with Next Generation RNA Sequencing (TRAPseq) in the *Fgf20* lineage.

Results: We show that TRAPseq targeting OC progenitors effectively enriched for RNA from this rare cell population. TRAPseq identified differentially expressed genes (DEGs) downstream of FGF20, including *Etv4*, *Etv5*, *Etv1*, *Dusp6*, *Hey1*, *Hey2*, *Heyl*, *Tectb*, *Fat3*, *Cpxm2*, *Sall1*, *Sall3*, and cell cycle regulators such as *Cdc20*. Analysis of *Cdc20* conditional-null mice identified decreased cochlea length, while analysis of *Sall1*-null and *Sall1*- *Zn2-10* mice, which harbor a mutation that causes Townes-Brocks syndrome, identified a decrease in outer hair cell number.

Conclusions: We present two datasets: genes with enriched expression in OC progenitors, and DEGs downstream of FGF20 in the embryonic day 14.5 cochlea. We validate select DEGs via in situ hybridization and in vivo functional studies in mice.

Keywords

cochlea; hair cell; RNAseq; SALL1; Townes-Brocks syndrome; hearing loss

INTRODUCTION

Congenital and acquired sensorineural hearing loss are common problems, yet there are no available biologically based therapies. Congenital sensorineural hearing loss can result from defects in sensory hair cells (HCs) or specialized supporting cells (SCs) within the organ of Corti (OC).¹⁻⁴ Acquired sensorineural hearing loss is commonly caused by damage to HCs.^{5,6} In mammals, HC loss is permanent as the mammalian OC is unable to regenerate HCs.^{5,7}

*Correspondence: 3905 South Bldg. (campus box 8103), Washington University School of Medicine, 660 S. Euclid Avenue, St. Louis, MO 63110, Telephone: (314) 362-3908, dornitz@wustl.edu.

One potential approach to treating hearing loss due to HC loss or damage is to reactivate developmental signaling pathways in latent progenitors to promote their growth and differentiation into HCs and SCs. Investigation of the developmental pathways regulating HC and SC differentiation will therefore benefit our understanding and treatment of both congenital and acquired hearing loss.

In mouse cochlea development, Fibroblast Growth Factor 20 (FGF20) signaling via FGF receptor 1 (FGFR1) is required for the differentiation of OC progenitors (prosensory cells) into HCs and SCs, specifically outer hair cells (OHCs) and outer supporting cells.⁸⁻¹² *Fgf20*-null mice (*Fgf20*^{-/-}) are deaf, with shorter cochleae and loss of OHCs and gaps of undifferentiated cells along the length of the OC interrupting the normal patterning of HCs and SCs.⁹ FGF20 is required during the initiation of HC and SC differentiation and *Fgf20*^{-/-} mice additionally exhibit premature onset of HC differentiation, as well as delayed apical progression of HC differentiation and maturation.^{9,13} We do not know the mechanism by which FGF20 is required for the initiation of differentiation. We hypothesize that downstream genetic targets of FGF20 signaling in prosensory cells will be candidate effectors of HC and SC differentiation. Identifying these genes will be important for advancing therapeutics in regenerating lost or damaged HCs and will provide insight into the mechanisms underlying OC phenotypes in *Fgf20*^{-/-} mice.

Here, we combined the Translating Ribosome Affinity Purification (TRAP) technology with Next Generation RNA Sequencing (TRAPseq) to study changes in gene expression patterns in prosensory cells in the presence or absence of FGF20 signaling in mice.¹⁴ TRAP allows the isolation of translating mRNA, as well as noncoding RNA bound to ribosomes, from specific cell populations without cell sorting or fine dissection.¹⁵ We used the *ROSA*^{fsTRAP} allele,¹⁵ which when activated by Cre recombinase leads to the expression of a GFP-tagged ribosomal protein (L10a-eGFP). Immunoprecipitation (IP) with anti-GFP antibodies then enriches for polysomes and associated RNA. We show that by targeting the expression of L10a-eGFP to prosensory cells within the cochleae in vivo using *Fgf20*^{Cre}, we were able to enrich for RNA within this relatively rare cell population. Comparing control and *Fgf20*^{-/-} prosensory cell RNA, TRAPseq revealed many genes previously associated with FGF signaling, as well as genes with functional significance in cochlea development. Among these genes is *Sall1*, mutations of which in humans cause Townes-Brocks syndrome, a genetic condition associated with variable features that include sensorineural hearing loss.^{16,17}

RESULTS

***Fgf20*^{Cre} targets L10a-eGFP expression to the prosensory domain and Kölliker's organ**

At embryonic day 14.5 (E14.5), the floor of the cochlear duct can be divided into three sections (Fig. 1A): 1) prosensory domain (PD), which contains prosensory cells that differentiate into HCs and SCs of the OC; 2) outer sulcus (OS), epithelium that is lateral (abneural) to the prosensory domain, which develops into the lesser epithelial ridge (LER), and 3) Kölliker's organ (KO), epithelium that is medial (neural) to the prosensory domain, which develops into the greater epithelial ridge (GER). At E14.5, *Fgf20* is expressed in the

prosensory domain and at postnatal day 1 (P1), the *Fgf20^{Cre}* lineage includes the OC and the GER.^{9,10}

To evaluate the TRAP technique for the *Fgf20* lineage, we combined the *ROSA^{fsTRAP}* and *Fgf20^{Cre}* alleles. The *Fgf20^{Cre}* allele was made by targeted insertion of a sequence encoding a GFP-Cre fusion protein replacing exon 1 of *Fgf20*.¹⁰ As expected, based on prior expression and lineage tracing experiments, at E14.5, L10a-eGFP fluorescence (green) from *Fgf20^{Cre/+}; ROSA^{fsTRAP/+}* cochleae was found in the prosensory domain, Kölliker's organ, the cochlear duct wall more medial to the Kölliker's organ, and some cells in the spiral ganglion (Fig. 1B). Also as expected, at P0, L10a-eGFP in *Fgf20^{Cre/+}; ROSA^{fsTRAP}* cochleae was found in the OC, the GER, and the region more medial to the GER (Fig. 1B).

Another *Fgf20*-null allele, *Fgf20^{βgal}*, was made by targeted insertion of a sequence encoding β-Galactosidase replacing exon 1 of *Fgf20*.⁹ We combined the *Fgf20^{Cre}* and *Fgf20^{βgal}* alleles to generate *Fgf20^{-/-}* mice (*Fgf20^{Cre/βgal}*), which maintained the same dosage of Cre as control mice (*Fgf20^{Cre/+}*). Importantly, based on double fluorescence expression from the *ROSA^{mTmG}* Cre-reporter allele, the *Fgf20^{Cre}* lineage (green) did not change in *Fgf20^{Cre/βgal}* compared to *Fgf20^{Cre/+}* cochleae (Fig. 1C). Based on these results, we concluded that *Fgf20^{Cre/+}; ROSA^{fsTRAP/+}* and *Fgf20^{Cre/βgal}; ROSA^{fsTRAP/+}* mice will allow enrichment for prosensory cell RNA, increasing the sensitivity of RNAseq to identify changes in gene expression within these cells in the absence of FGF20 signaling.

***Fgf20^{Cre}* TRAPseq enriched for prosensory domain RNA**

TRAP experiments were performed at E14.5 (Fig. 1D), based on our previous findings that FGF20 signaling is required for prosensory cell differentiation at E13.5-E15.5.¹³ In the initial experiment, we collected pre-TRAP (pre-IP) and TRAP (post-IP) RNA from *Fgf20^{Cre/+}; ROSA^{fsTRAP/+}* cochleae at E14.5. Pre-TRAP samples were collected prior to IP, representing whole cochlea RNA, including RNA from mesenchyme and otic capsule (Fig. 1E). Quantitative reverse transcription PCR (qRT-PCR) showed enrichment of the prosensory cell marker *Id2* and depletion of the mesenchyme marker *Twist2* (also called *Dermo1*) in TRAP RNA samples, compared to pre-TRAP RNA samples (Fig. 1F).^{10,18}

Next, we performed TRAPseq with *Fgf20^{-/+}* (*Fgf20^{Cre/+}; ROSA^{fsTRAP/+}*) control and *Fgf20^{-/-}* (*Fgf20^{Cre/βgal}; ROSA^{fsTRAP/+}*) E14.5 cochleae. *Fgf20^{-/+}* and *Fgf20^{-/-}* embryos were generated at a 1:1 ratio. For each litter, cochleae from all control embryos were pooled together for RNA collection, and likewise for *Fgf20^{-/-}* embryos. Each sample represents RNA from pooled tissue from a minimum of three embryos. In total, 24 libraries were sequenced, consisting of 16 TRAP samples (8 *Fgf20^{-/+}* and 8 *Fgf20^{-/-}*) and 8 pre-TRAP samples (4 *Fgf20^{-/+}* and 4 *Fgf20^{-/-}*). See Experimental Procedures for details.

Principal component analysis (PCA) of the 24 RNAseq samples showed separation between pre-TRAP and TRAP samples along PC1 (Fig. 2A). However, there was no separation between *Fgf20^{-/+}* vs. *Fgf20^{-/-}* samples along PC1 or PC2. PCA of only the 16 TRAP samples also did not show separation between *Fgf20^{-/+}* vs. *Fgf20^{-/-}* samples along the first two PCs (Fig. 2B). To assess the efficiency of the TRAP technique, differentially expressed gene (DEG) analysis using DESeq2 was performed to compare pre-TRAP control samples

with TRAP control samples (same genotype, *Fgf20^{Cre/+};ROSA^{fsTRAP/+}*, for both).¹⁹ 3850 DEGs were identified with adjusted p-value (padj) < 0.01 and Log₂ Fold Change (LFC) < -1 or > 1 (Fig. 2C). Of these, 2017 genes had decreased expression in TRAP samples, compared to pre-TRAP (depleted by TRAP) and 1833 genes had increased expression in TRAP samples, compared to pre-TRAP (enriched by TRAP). Among the genes depleted by TRAP were mesenchymal markers *Cd44* and *Twist2*,^{10,20} vasculature markers *Eln* and *Fbln1*,^{21,22} and chondrocyte markers *Runx2* and *Matn1*.^{23,24} This was expected, since periotic mesenchyme and otic capsule were included in the input tissue but did not express L10a-eGFP. *Bmp4*, *Lmx1a*, and *Gata2*, markers of the outer sulcus were depleted as well.^{25,26} This was also expected, as the outer sulcus also did not express L10a-eGFP (Fig. 1A, B). Among the genes enriched by TRAP were prosensory domain markers *Fgf20*, *Atoh1*, *Hey2*, *Sox2*, *Gata3*, and *Id2*,^{9,18,27-30} Kölliker's organ markers *Lfng*, *Fgf10*, and *Jag1*,²⁶ and spiral ganglion markers *Neurod1* and *Tubb3*,^{31,32} all as expected. Gene set overlap analysis with gene ontology (GO) on genes depleted by TRAP showed biological processes terms "angiogenesis" and "endochondral ossification" among the top terms (Table 1). GO analysis on genes enriched by TRAP showed biological processes terms "sensory perception of sound", "axon guidance", and "auditory receptor cell stereocilium organization" among the top terms (Table 2). These results strongly suggest that TRAP enriched for RNA from *Fgf20^{Cre}*-lineage cells.

Pre-TRAP vs. TRAP DEG analysis data are presented in Supplemental file S1. The top 50 GO terms from GO analysis on genes depleted by TRAP vs. pre-TRAP (2017 DEGs with LFC < -1 and padj < 0.01) are presented in Supplemental file S2. The top 50 GO terms from GO analysis on genes enriched by TRAP vs. pre-TRAP (1833 DEGs with LFC > 1 and padj < 0.01) are represented in Supplemental file S3. In the following text, we focus on the *Fgf20^{-/+}* vs. *Fgf20^{-/-}* TRAPseq DEG analysis. We refer to the TRAP vs. pre-TRAP DEG analysis with terms "enriched by TRAP" and "depleted by TRAP." "Enriched by TRAP" refers to transcripts with increased abundance in TRAP relative to pre-TRAP RNA from *Fgf20^{Cre/+};ROSA^{fsTRAP/+}* cochleae; "depleted by TRAP" refers to transcripts with decreased abundance in TRAP relative to pre-TRAP RNA from *Fgf20^{Cre/+};ROSA^{fsTRAP/+}* cochleae.

TRAPseq revealed known FGF target genes during organ of Corti differentiation downstream of *Fgf20*

DEG analysis on *Fgf20^{-/+}* vs. *Fgf20^{-/-}* pre-TRAP samples resulted in, as expected, very few DEGs. In fact, there were only three DEGs with padj < 0.1: *Tectb*, *Calb1*, and *Fgf20* (data not shown). DEG analysis on *Fgf20^{-/+}* vs. *Fgf20^{-/-}* TRAP samples resulted in 47 DEGs with padj < 0.01 and 104 DEGs with padj < 0.1 (Fig. 3A). GO analysis with the top 362 TRAPseq DEGs (cut-off of padj < 0.5) found among the top 40 terms "sensory perception of sound," "sensory organ morphogenesis," "ear development," and "inner ear receptor cell differentiation" (Table 3). Many neuronal and cell cycle biological processes terms, such as "regulation of neuron differentiation," "forebrain neuron differentiation," "regulation of neural precursor cell proliferation," "cell division," and "cell cycle arrest" were also among the top terms. *Fgf20^{-/+}* vs. *Fgf20^{-/-}* DEG analysis data are presented in Supplemental file

S4. The top 50 GO terms from GO analysis on 362 DEGs with $\text{padj} < 0.5$ are presented in Supplemental file S5.

For *Fgf20*^{-/+} vs. *Fgf20*^{-/-} TRAPseq DEG analysis, we considered $\text{padj} < 0.1$ to be statistically significant. Confirming the validity of the TRAPseq data, DEGs with $\text{padj} < 0.1$ included *Fgf20* as well as *Hey1*, *Hey2*, *Etv4*, and *Etv5* (Table 4), which we have previously shown by RNA in situ hybridization (ISH) are downregulated in *Fgf20*^{-/-} vs. *Fgf20*^{-/+} cochleae.¹³ To confirm other DEGs identified by TRAPseq, we examined their expression patterns via ISH in *Fgf20*^{-/+} (*Fgf20*^{Cre/+}) and *Fgf20*^{-/-} (*Fgf20*^{Cre/ β gal}) E14.5 cochleae.

We began with DEGs that have been well-linked to FGF signaling (Table 4) and were downregulated in *Fgf20*^{-/-} cochleae, such as *Dusp6*, *Etv1*, *Spry1*, and *Spry4* (Fig. 3B).³³⁻³⁶ By ISH, *Dusp6* (Dual specificity phosphatase 6) was expressed within the prosensory domain in control cochleae, and was almost undetectable in *Fgf20*^{-/-} cochleae. *Etv1* (Ets variant 1) was also expressed within the prosensory domain. Interestingly, while *Etv1* expression was absent in the prosensory domain in *Fgf20*^{-/-} cochleae, it was increased in the outer sulcus (Fig. 3B, arrowhead). *Spry1* (Sprouty homolog 1) expression was found in the prosensory domain and outer sulcus, similar to *Etv1*, *Etv4*, and *Etv5* expression at this stage.¹³ In *Fgf20*^{-/-} cochleae, *Spry1* was absent from the prosensory domain, but not the outer sulcus, similar to the change in expression patterns of *Etv4* and *Etv5* in *Fgf20*^{-/-} cochleae.¹³ *Spry4* (Sprouty homolog 4) expression was found more diffusely in the floor of the cochlear duct, and appeared slightly decreased in the prosensory domain of *Fgf20*^{-/-} cochleae, although it was difficult to tell definitively by ISH.

TRAPseq revealed many genes associated with cochlea development or hearing loss downstream of *Fgf20*

Many DEGs from *Fgf20*^{-/+} vs. *Fgf20*^{-/-} TRAPseq have previously been associated with cochlea development (Table 5). We validated some interesting DEGs via ISH, including *Tectb*, *Smpx*, *Epyc*, *Fat3*, and *Hey1*, the results of which were all consistent with TRAPseq data (Fig. 4A). *Tectb* (Tectorin beta) was expressed in the prosensory domain and Kölliker's organ and was nearly absent in the prosensory domain of *Fgf20*^{-/-} cochleae. Meanwhile, *Tecta* (Tectorin alpha), which also trended towards lower expression per TRAPseq, but did not meet the padj cut-off ($\text{padj} = 0.22$), was not differentially expressed based on ISH. *Smpx* (Small muscle protein, X-linked) was lowly expressed in the prosensory domain and was increased in *Fgf20*^{-/-} cochleae. *Epyc* (Epiphycan) was faintly expressed in the medial cochlear duct wall at this stage and was increased in *Fgf20*^{-/-} cochleae. *Fat3* (FAT atypical cadherin 3) was expressed in the prosensory domain and was decreased in *Fgf20*^{-/-} cochleae. *Hey1* (hairly/enhancer-of-split related with YRPW motif-like), belonging to the same family as *Hey1* and *Hey2*, was not expressed in *Fgf20*^{-/+} cochleae at E14.5, but was detected in the prosensory domain in *Fgf20*^{-/-} cochleae.

TRAPseq also identified a few transcription factors that were depleted by TRAP, but with increased expression in *Fgf20*^{-/-} cochleae, including *Gata2* (GATA binding protein 2), *Meis2* (Meis homeobox 2), and *Lmx1a* (LIM homeobox transcription factor 1 alpha). Depletion by TRAP suggests that they are not highly expressed in the prosensory domain or Kölliker's organ. By ISH, all three genes were expressed in the outer sulcus and/or roof of

the cochlear duct (Fig. 4B). However, ISH did not appear to be sensitive enough to detect differences in the expression of any of these genes between *Fgf20*^{-/+} and *Fgf20*^{-/-} cochleae. *Bmp4* (Bone morphogenetic protein 4) was also depleted by TRAP, but not significantly changed in *Fgf20*^{-/-} cochleae per TRAPseq (padj = 0.38). By ISH *Bmp4* was expressed in the outer sulcus and did not show any changes in *Fgf20*^{-/-} compared to *Fgf20*^{-/+} cochleae (Fig. 4B).

TRAPseq revealed decreased expression of cell cycle regulators in the absence of *Fgf20*

GO analysis on *Fgf20*^{-/+} vs. *Fgf20*^{-/-} TRAPseq DEGs showed that the cell cycle may be affected by the loss of FGF20, with “cell division” and “cell cycle arrest” among the top terms (Table 3). This was confirmed by known and predicted protein-protein interaction (PPI) network identification via the STRING database with the top 192 DEGs, representing those with padj < 0.3.^{37,38} By far the largest PPI network identified consisted of cell cycle regulators (Fig. 5A). The list of top DEGs indeed showed many genes involved in cell cycle regulation, all of which were decreased in expression in *Fgf20*^{-/-} cochleae (Table 6).

Although we have not found that *Fgf20* regulates cell cycle progression by itself, *Fgf20* does interact with *Fgf9* and *Sox2* to regulate prosensory progenitor and Kölliker’s organ proliferation, respectively.^{10,13} We hypothesize, therefore, that the expression changes in cell cycle regulators may reflect these functions of *Fgf20*. To rule out the possibility that cell cycle regulation contributes to the differentiation and patterning defect found in *Fgf20*^{-/-} cochleae, we examined the largest hub of the PPI network, *Cdc20* (Cell division cycle 20). *Cdc20* is a coactivator of the anaphase-promoting complex (APC), the cell cycle-regulated ubiquitin ligase. Interestingly, Cdc20-APC is required for presynaptic axon differentiation in postmitotic neurons in the cerebellum.³⁹

By ISH, *Cdc20* is expressed diffusely throughout the developing cochlear duct epithelium at E12.5 (Fig. 5B). By E14.5, its expression is decreased within the prosensory domain (Fig. 5B, brackets), corresponding with prosensory cell cycle exit.^{40,41} There was no consistently detectable difference in *Cdc20* expression between *Fgf20*^{-/+} and *Fgf20*^{-/-} cochleae at E12.5 or E14.5 by ISH.

To examine whether *Cdc20* may be involved in HC differentiation, we combined the *Fgf20*^{Cre} and *Cdc20*^{lox} alleles to conditionally delete *Cdc20* from the *Fgf20*^{Cre} lineage.⁴² *Fgf20*^{Cre} targets parts of the otic epithelium as early as E10.5,¹⁰ and by E12.5 targets the medial parts of the cochlear duct floor epithelium (Fig. 5C), similar to E14.5 (Fig. 1C). *Fgf20*^{Cre/+}; *Cdc20*^{lox/lox} (*Cdc20*^{CKO}) cochleae (length: 3.48 ± 0.75 mm) were shorter and more tightly coiled than *Fgf20*^{Cre/+}; *Cdc20*^{lox/+} (*Cdc20*^{CHet}) cochleae (length: 4.86 ± 0.18 mm) (Fig. 5D, F). Importantly, HCs (labeled by phalloidin, green) in *Cdc20*^{CKO} cochleae exhibited the normal pattern of one row of IHCs separated from three rows of OHCs by pillar cells (inner pillar cells labeled by P75^{NTR}, red) (Fig. 5E). Interestingly, 4 of 5 *Cdc20*^{CKO} cochleae examined had 4 or more rows of OHCs at the apical tip (Fig. 5E), which may be the result of a defect in convergent extension. The tighter coil and convergent extension defect found in *Cdc20*^{CKO} cochleae may be attributable to the loss of *Cdc20* expression from the Kölliker’s organ and medial cochlear duct wall. Upon quantification, total number of IHCs and OHCs were decreased in *Cdc20*^{CKO} (IHC: 339 ± 59; OHC: 1295

± 108) relative to *Cdc20^{CHet}* (IHC: 580 ± 9 ; OHC: 1916 ± 59) cochleae (Fig. 5F); however, this can likely be attributed to the shorter cochlea length.

***Sall1* mutant cochleae exhibit an outer hair cell phenotype**

Sall1 (Sal-like 1) and *Sall3* (Sal-like 3), members of a family of transcription factors, are expressed in the cochlear duct throughout development.⁴³⁻⁴⁶ Both were identified by TRAPseq as decreased in *Fgf20^{-/-}* cochleae compared to *Fgf20^{+/+}* (Table 5). ISH showed that both *Sall1* and *Sall3* were expressed in the prosensory domain and were decreased in *Fgf20^{-/-}* cochleae (Fig. 6A). *Sall2* (Sal-like 2), another member of the same family, trended towards lower expression per TRAPseq (padj = 0.26). By ISH, *Sall2* was also expressed in the prosensory domain, but was not noticeably decreased in *Fgf20^{-/-}* cochleae (Fig. 6A). *Sall4*, the remaining member of the *Sall* family, was filtered out from TRAPseq DEG analysis due to insufficiently low read counts.

Importantly, *SALL1* has been linked to Townes-Brocks syndrome (TBS) in humans, which causes sensorineural hearing loss, among other developmental defects.¹⁶ Mutations in one copy of *SALL1* is responsible for TBS, although *SALL1* haploinsufficiency may not be the sole causative factor, as *Sall1*-null mice do not recapitulate the human TBS phenotypes.⁴³ Instead, mice expressing one copy of a *Sall1* allele with mutations known to cause TBS, *Sall1- Zn2-10* (*Sall1*), mimic TBS defects, including hearing loss.⁴⁷ This mutation results in a truncated protein encoding the N-terminus of Sall1, which has been shown to mediate transcriptional repression.⁴⁸ Like wildtype Sall1, the truncated Sall1 protein can bind all members of the Sall family,⁴⁷ and its expression alone in transgenic mice leads to derepression of Sall-regulated genes, resulting in TBS-like phenotypes.⁴⁹ These results suggest that Sall1 may act as a dominant negative and interfere with the transcription-repressor activity of all Sall proteins.

To investigate whether *Sall1* may have a role in HC differentiation, we examined *Sall1*-null (*Sall1^{-/-}*) cochleae along with cochleae from littermate controls (*Sall1^{+/+}* and *Sall1^{-/+}*) at E18.5.⁵⁰ HC patterning in *Sall1^{-/+}* and *Sall1^{-/-}* cochleae appeared similar to that in *Sall1^{+/+}* cochleae, with mostly one row of IHCs and three rows of OHCs throughout the entire cochlear duct (Fig. 6B). Upon quantification of cochlea length, *Sall1^{-/-}* cochleae (5.59 ± 0.17 mm) were found to be slightly but statistically significantly shorter than *Sall1^{+/+}* (6.26 ± 0.43 mm) but not *Sall1^{-/+}* (5.94 ± 0.36 mm) cochleae (Fig. 6C). While the total number of IHCs did not significantly differ among the three genotypes (*Sall1^{+/+}*: 676 ± 20 ; *Sall1^{-/+}*: 701 ± 8 ; *Sall1^{-/-}*: 674 ± 19), the total number of OHCs was significantly decreased in *Sall1^{-/-}* cochleae (2053 ± 43) compared to both *Sall1^{+/+}* (2342 ± 66) and *Sall1^{-/+}* (2308 ± 43) cochleae (Fig. 6C). These results suggest that there is an OHC-specific developmental defect in *Sall1^{-/-}* cochleae.

Interestingly, many ectopic IHCs (found outside of the normal row of IHCs) were present along the entire length of the *Sall1^{-/-}* cochleae, especially towards the apex (Fig. 6B, arrowheads). Upon quantification, the total number of ectopic IHCs was significantly increased in *Sall1^{-/-}* cochleae (21 ± 8) compared to *Sall1^{+/+}* cochleae (7 ± 5) (Fig. 6C). The number of ectopic IHCs was also increased in *Sall1^{-/-}* cochleae compared to *Sall1^{-/+}*

cochleae (9 ± 6), but this was not statistically significant (Fig. 6C). This finding suggests a sensory epithelium patterning defect in *Sall1*^{-/-} cochleae.

We hypothesized that the dominant negative effects of *Sall1* may recapture the effects of decreased *Sall1* and *Sall3* expression found in *Fgf20*^{-/-} cochleae, producing a phenotype more severe than that of *Sall1*^{-/-} cochleae and more similar to that of *Fgf20*^{-/-} cochleae. We examined cochleae from mice heterozygous (*Sall1*^{+/-}) and homozygous (*Sall1*^{/-}) for the *Sall1* mutation, as well as from wildtype littermate controls (*Sall1*^{+/+}) at E18.5.⁴⁷ Most *Sall1*^{/-} embryos die by E16.5.⁴⁷ However, we were able to obtain three *Sall1*^{/-} embryos that survived to E18.5 (3/84 total embryos across 10 litters, with expected ratio of 1/4). Similar to *Sall1*^{-/-} cochleae, the overall HC patterning appeared relatively unchanged in *Sall1*^{+/-} and *Sall1*^{/-} cochleae compared to *Sall1*^{+/+} cochleae (Fig. 7A).

Upon quantification of cochlea length, *Sall1*^{/-} cochleae (4.92 ± 0.84 mm) were found to be slightly but statistically significantly shorter than both *Sall1*^{+/+} (6.09 ± 0.25 mm) and *Sall1*^{+/-} (5.75 ± 0.50 mm, including a possible outlier at 4.65 mm) cochleae (Fig. 7B). The total number of IHCs appeared to be slightly decreased in *Sall1*^{/-} cochleae (664 ± 50) compared to *Sall1*^{+/+} (709 ± 21) and *Sall1*^{+/-} (702 ± 31) cochleae, but this was not statistically significant. Notably, the total number of OHCs was significantly decreased in *Sall1*^{+/-} cochleae (2311 ± 80) compared to *Sall1*^{+/+} cochleae (2478 ± 79), and was further significantly decreased in *Sall1*^{/-} cochleae (1969 ± 111) (Fig. 7B).

Similar to *Sall1*^{-/-} cochleae, many ectopic IHCs were found throughout the length of *Sall1*^{/-} cochleae, especially towards the apex (Fig. 7A, arrowheads). Quantification of these ectopic IHCs showed a statistically significant increase in *Sall1*^{/-} (45 ± 19) compared to *Sall1*^{+/+} (7 ± 4) and *Sall1*^{+/-} (10 ± 7) cochleae (Fig. 7B).

In addition, the HCs in *Sall1*^{/-} cochleae appeared less mature than those found in comparative regions of *Sall1*^{+/+} and *Sall1*^{+/-} cochleae based on F-actin organization in phalloidin stained samples (Fig. 7A, inset). This was most apparent in the mid-apical turns, where stereocilia bundles appeared relatively well-formed in *Sall1*^{+/+} and *Sall1*^{+/-} cochleae (arrows in Fig. 7A, inset). In *Sall1*^{/-} cochleae, however, the stereocilia in this region appeared more immature and disorganized (arrow in Fig. 7A inset), resembling those found in the less mature apical tip [HC differentiation and maturation occur in a base-to-apex gradient,² therefore, more apical HCs are less mature]. In the apical tip, the F-actin networks at the HC cortex in *Sall1*^{/-} cochleae appeared less dense than those found in *Sall1*^{+/+} and *Sall1*^{+/-} cochleae, as indicated by weaker phalloidin labeling (Fig. 7A, inset).

Overall, the *Sall1*^{/-} phenotype is similar to, but more severe than the *Sall1*^{-/-} phenotype. Compared to their respective littermate *Sall1*^{+/+} cochleae, *Sall1*^{-/-} cochleae were 10.7% shorter, while *Sall1*^{/-} cochleae were 19.2% shorter. *Sall1*^{-/-} cochleae had a 12.3% decrease in total OHC number, while *Sall1*^{/-} cochleae had a 20.5% decrease in total OHC number. *Sall1*^{-/-} cochleae had a 300% increase in the number of ectopic IHCs, while *Sall1*^{/-} cochleae had a 643% increase in the number of ectopic IHCs.

DISCUSSION

We have adapted the TRAP technique to study a relatively small population of difficult-to-isolate cells: cochlear prosensory cells. TRAP using *Fgf20^{Cre}* combined with *ROSA^{flsTRAP}* effectively enriched for RNA from the *Fgf20^{Cre}* lineage at E14.5. We believe the pre-TRAP vs. TRAP DEG analysis provides a useful dataset for identifying genes enriched in the prosensory domain, Kölliker's organ, and spiral ganglion of the developing cochlea.

TRAPseq DEG analysis comparing *Fgf20^{+/+}* and *Fgf20^{-/-}* E14.5 cochlea samples showed decreased expression of known FGF20 signaling targets in the cochlea at this stage, as well as known FGF signaling targets in other tissues, confirming the validity of the TRAP technique. Just as importantly, TRAPseq DEGs did not include genes that we have previously shown are not downstream of FGF20, but that have been shown to be downstream of FGFR1: *Cdkn1b* and *Sox2* (Table 5).^{10,11,13} Interestingly, *Lockd*, a non-coding RNA near the *Cdkn1b* locus and co-expressed with *Cdkn1b*,⁵¹ was significantly decreased in *Fgf20^{-/-}* cochleae (Table 5). The expression of a few other genes previously shown to be downstream of FGFR1 during cochlea development, such as *Fgf10*, *Hes5*, and *Ntf3*,^{11,12} were also not significantly changed in *Fgf20^{-/-}* compared to *Fgf20^{+/+}* cochleae. MAP3K4 (also called MEKK4) activity has been associated with FGF20-FGFR1 signaling during hair cell differentiation.⁵² However, while MAP3K4 protein levels were previously shown to be decreased in *Fgf20^{-/-}* relative to *Fgf20^{+/+}* cochleae at P0, *Map3k4* transcript levels were not changed in *Fgf20^{-/-}* compared to *Fgf20^{+/+}* cochleae at E14.5, per TRAPseq.

As with any large data experiment, false positives and negatives are expected. Here, we used a lenient false discovery rate of 0.1 to evaluate *Fgf20^{+/+}* vs. *Fgf20^{-/-}* TRAPseq results to reduce the number of false negatives at the cost of increasing false positives. While we were able to confirm many TRAPseq DEGs via ISH, as well as confirm the expression of several non-significantly changed genes as unchanged via ISH, there were discrepancies between TRAPseq and ISH results. Besides false positivity, another possible and interesting explanation for the discrepancies is that TRAPseq specifically identifies differences in ribosome-bound RNA. Such differences may not always be reflected in the whole RNA population detected by ISH.

Another caveat is that the *Fgf20^{Cre}*-TRAP enrichment process is not perfect, due to technical limitations and the inclusion of Kölliker's organ and spiral ganglion cells in the *Fgf20^{Cre}* lineage. RNA from these sources dilute the RNA from the target prosensory cell population, reducing the power of TRAPseq in detecting changes within this population.

TRAPseq identified DEGs previously associated with cochlea development or hearing downstream of *Fgf20*

Many DEGs identified by *Fgf20^{+/+}* vs. *Fgf20^{-/-}* TRAPseq have known roles in cochlea development (Table 5). Altered expression of these genes, therefore, may contribute to the *Fgf20^{-/-}* phenotype. Importantly, we do not know what proportion of these DEGs are directly regulated by FGF20, and what proportion may be indirectly regulated or are markers of dysregulated differentiation. Here, we highlight some of these DEGs.

Fat3 (FAT atypical cadherin 3), encoding a mammalian homolog of the *Drosophila* cell adhesion molecule Fat, is required for the normal patterning of OHCs, along with *Fat4*.⁵³ *Fat3*-null cochleae exhibits a small loss of OHCs from the base of the cochlea and a slight gain of OHCs in the mid-apex. We hypothesize that the decreased expression of *Fat3* may contribute to the OHC patterning defect in *Fgf20*^{-/-} cochleae.

Cpxm2 (Carboxypeptidase X 2) is one of the three genes on chromosome 7 deleted in the head bobber mouse line, which exhibits deafness and vestibular defects.^{54,55} However, how *Cpxm2* deletion contributes to deafness in these mice has not been elucidated.

Tectb (Tectorin beta) is expressed in the prosensory domain and encodes a major glycoprotein in the tectorial membrane required for normal hearing.^{56,57} Interestingly, *Tecta*, another gene encoding a glycoprotein in the tectorial membrane, trended towards lower expression (not statistically significantly) but did not show decreased expression by ISH. The composition of the tectorial membrane in *Fgf20*^{-/-} cochleae has not been studied.

Thrb (Thyroid hormone receptor beta) is expressed in the OC, GER, spiral ligament, and spiral ganglion in the neonatal cochlea. *Thrb*-mutant mice (both null and mutants with disrupted thyroid hormone binding) have severe hearing loss attributed to disruption of postnatal morphogenesis of the tectorial membrane.⁵⁸⁻⁶² Interestingly, *Thrb* trended towards increased expression per TRAPseq (padj = 0.13).

Myh14 (Myosin, heavy polypeptide 14) is one of the genes encoding Myosin II. It is expressed in both developing HCs and SCs in the prenatal OC. Myosin II is required for patterning and convergent extension in the cochlea.⁶³ A convergence and extension defect may contribute to the shortened length of *Fgf20*^{-/-} cochleae. *Myh14* trended towards decreased expression per TRAPseq (padj = 0.23).

Smpx (Small muscle protein, X-linked), previously shown to be expressed in HCs,⁶⁴ is associated with heritable progressive hearing loss.⁶⁵⁻⁶⁷ However, *Smpx*-null mice have not been shown to have a hearing defect or much of an overt developmental phenotype.⁶⁸ Given that *Smpx* is expressed in HCs, its increased expression in the prosensory domain of *Fgf20*^{-/-} cochleae may reflect the premature onset of HC differentiation in these mice.

Epyc (Epiphycan), encoding a proteoglycan expressed in mature nonsensory regions of the cochlear duct, is required for normal hearing.⁶⁹ Its increased expression in *Fgf20*^{-/-} cochleae may also reflect premature onset of differentiation, although it has not been shown that the Kölliker's organ and medial cochlear duct wall undergoes premature differentiation in *Fgf20*^{-/-} cochleae.

Hey1 and *Hey2* (hairy/enhancer-of-split related with YRPW motif 1 and 2) have been shown to be downstream of FGF20 signaling in the developing cochlea and are required to prevent premature HC differentiation.^{13,70} Unlike *Hey1* and *Hey2*, *Hey1* is not expressed in the prosensory domain at E14.5. However, it can be detected in the developing Kölliker's organ and differentiating supporting cells in the prosensory domain at E16.5 through at least P0.⁷¹⁻⁷³ The increased expression of *Hey1* in *Fgf20*^{-/-} cochleae may also reflect premature onset of differentiation. Additionally, *Fgf20* expression in the developing OC decreases as

HCs differentiate,⁹ corresponding with the onset of *Hey1* expression. This suggests that *Fgf20* may inhibit *Hey1* expression directly. Notably, *Hey1*^{-/-} mice have a normal number of organ of Corti HCs at P0.⁷² However, the exact role of *Hey1* in cochlea development has not been elucidated. It is further unclear what effect ectopic/premature expression of *Hey1* in the prosensory domain may have on OC differentiation.

TRAPseq identified DEGs with unknown functions in cochlea development downstream of *Fgf20*

Most of the DEGs identified by *Fgf20*^{+/-} and *Fgf20*^{-/-} TRAPseq have no known roles in cochlea development. However, some of these are related to genes with known roles in cochlea development, suggesting possible redundancy. Here, we highlight some of the most interesting ones.

Dusp6 (Dual specificity phosphatase 6) is a known downstream target of FGF signaling and is a downstream target of FGF20 signaling in the olfactory system.^{36,74} Mice heterozygous for a *Dusp6*-null allele exhibit hearing loss, attributed to malformed otic capsule and ossicles.⁷⁵ While *Dusp6* is known to be expressed in the prosensory domain and the OC,⁷⁶ which we confirm, its role in the development of these structures has not been investigated.

Etv4 (Ets variant 4) and *Etv5* (Ets variant 5) have been shown to be downstream of FGF20/FGFR1 signaling in the developing cochlea.^{8,13} However, *Etv1*, the third member of the PEA3 group of Ets transcription factors, has not been associated with cochlea development. We show here that *Etv1* expression is decreased in the prosensory domain in *Fgf20*^{-/-} cochleae, while its expression is increased in the outer sulcus. This is potentially a significant pattern change, as the *Fgf20*^{-/-} phenotype is more severe in the outer compartment of the OC, directly adjacent to the outer sulcus/LER. Investigating whether this increase in expression in the outer sulcus contributes to the *Fgf20*^{-/-} phenotype will be addressed in future experiments.

Other DEGs with unclear functional significance but that are known to be expressed in the cochlea include the following (Table 5):

- *Pou3f3* (POU domain, class 3, transcription factor 3): expressed in SCs and mesenchymal cells in the cochlea.⁷⁷ Based on ISH from the Eurexpress atlas, it is also expressed in the cochlear duct floor at E14.5 (http://www.eurexpress.org/euxassay_019559).⁷⁸ However, analysis of the *Pou3f3*-null mouse cochlea did not reveal any apparent developmental defects.⁷⁷ Despite this, auditory and vestibular impairments have been reported in a *Pou3f3* (*Pou3f3*^{L423P}) mutant mouse line.⁷⁹ Interestingly, the expression of *Pantr1* (*Pou3f3* adjacent noncoding transcript 1), a lncRNA that shares a bidirectional promoter with *Pou3f3*,⁸⁰ was also decreased in *Fgf20*^{-/-} cochleae per TRAPseq, suggesting disrupted activity at the promoter. In addition, *Rorb* (RAR-related orphan receptor beta), found to be increased in *Fgf20*^{-/-} cochleae by TRAPseq, has an antagonistic interaction with *Pou3f3* during cell fate specification in the developing neocortex.⁸¹
- *Calb1* (Calbindin 1): expressed in mature HCs.⁸² Upregulation may represent premature onset of HC differentiation in *Fgf20*^{-/-} cochleae.

- *Crym* (Crystallin, mu): a thyroid hormone binding protein, highly expressed in nonsensory regions of the cochlea in adult rats.⁸³
- *Shc4* (SHC family, member 4): an adaptor protein expressed in the cochlear duct floor at E14.5 and E15.5.⁸⁴
- *Car13* (Carbonic anhydrase 13): expressed in nonsensory regions of the cochlea and the mesenchyme at E15.5 and neonatal stages.⁸⁵
- *Tac1* (Tachykinin 1): reported to be expressed in the cochlear epithelium during development.⁸⁶
- *Lum* (Lumican): expressed in the otic capsule, some mesenchyme, and nonsensory regions of the cochlear duct.⁸⁷
- *Nes* (Nestin): expressed in the spiral ganglion and parts of the prosensory domain at E14.5 and E15.5, as well as in mature SCs.^{88,89}

Nonsensory cell markers are upregulated in *Fgf20*^{-/-} cochleae

Fgf20^{+/-} vs. *Fgf20*^{-/-} TRAPseq also identified a few transcription factors expressed in the outer sulcus and other nonsensory cochlear epithelium: *Gata2*, *Meis2*, and *Lmx1a*.^{25,90-94} Interestingly, they were all increased in *Fgf20*^{-/-} cochleae per TRAPseq suggesting that undifferentiated progenitors in *Fgf20*^{-/-} cochlea may have adopted a nonsensory identity. Two other outer sulcus/nonsensory epithelial markers, *Hmx2* and *Bmp4*,^{95,96} also trended toward increased expression in *Fgf20*^{-/-} cochleae, albeit not significantly (padj = 0.11 and 0.38, respectively). *Bmp4* is interesting because of its importance in patterning the outer sulcus, prosensory domain, and Kölliker's organ.²⁶

Examining the expression of these genes by ISH did not reveal noticeable changes between *Fgf20*^{+/-} and *Fgf20*^{-/-} cochleae. We hypothesize that because TRAP depletes for the outer sulcus and roof of the cochlear duct, TRAPseq is highly sensitive to the expression of markers of these regions in the prosensory domain. Therefore, TRAPseq may be much more sensitive than ISH to detect small changes in the expression of genes such as *Gata2*, *Meis2*, and *Lmx1a*, which may represent a shift in the boundary between the prosensory domain and outer sulcus.

Cell cycle regulators are downregulated in *Fgf20*^{-/-} cochleae

TRAPseq revealed many differentially expressed cell cycle regulators. We have shown before that *Fgf20* by itself does not appear to regulate the cell cycle or proliferation in the developing cochlea. However, *Fgf20* is redundant with *Fgf9* in indirectly regulating prosensory progenitor proliferation at earlier developmental stages (E11.5-E12.5) and is redundant with *Sox2* in regulating Kölliker's organ proliferation at E14.5.^{10,13} Therefore, we believe the finding of differentially expressed cell cycle regulators may reflect the redundant and stage-specific functions of *Fgf20* in regulating proliferation. As expected, while *Cdc20* conditional-null cochleae are short, they do not exhibit the HC differentiation or patterning defect found in *Fgf20*^{-/-} cochleae. We conclude that the ~10-20% decrease in length of *Fgf20*^{-/-} cochleae may be attributable to decreased expression of these cell cycle regulators in sensory progenitors. It is also possible that *Fgf20* has a previously unidentified role in

regulating prosensory cell cycle exit, and decreased expression of these cell cycle regulator genes are reflective of premature cell cycle exit.

***Fgf20* is upstream of *Sall1*, a gene implicated in human sensorineural hearing loss**

We found that members of the *Sall* family, *Sall1*, *Sall2*, and *Sall3*, are expressed in the prosensory domain at E14.5, consistent with previous reports of *Sall1* and *Sall3* expression at around this stage.^{44,46} *Sall1*, *Sall3*, and potentially *Sall2* showed decreased expression by TRAPseq and ISH in *Fgf20*^{-/-} cochleae, suggesting that they are likely regulated by FGF20 signaling. Notably, in the kidney, *Sall1* expression has been shown to be regulated by FGF signaling.⁹⁷ As mentioned previously, mutations in *SALL1* causes Townes-Brocks syndrome (TBS) in humans, an autosomal dominant disorder with variable presentation of phenotypes including sensorineural hearing loss.¹⁶ *Sall1*^{+/+} mice mimic TBS developmental defects, including hearing loss.⁴⁷ Whether cochlea development is affected in *Sall1*^{-/-} and *Sall1* mice has not been reported.

We found that *Sall1*^{+/+} had relatively normal HC patterning, but exhibited a small decrease in the total number of OHCs. This is reminiscent of the *Fgf20*^{-/-} and *Fgf20,Sox2* compound mutant phenotypes, in which OHCs are the most sensitive to the loss of FGF20.^{9,13} We are not sure, however, how much this reduction in the number of OHCs contributes to the hearing defect found in these mice.

Sall1^{-/-} and *Sall1*^{+/+} cochleae both exhibited more severe developmental defects than *Sall1*^{+/+} cochleae, including shorter cochlea length, and larger decreases in the total number of OHCs. We do not know whether the decrease in HC number is solely attributable to the shorter length of these cochleae. It is possible that both the HC and cochlea length phenotypes are the result of a defect in prosensory progenitor proliferation, such as that found in *Fgf20, Fgf9* double mutant mice,¹⁰ or the result of a defect in prosensory specification, such as that found in *Sox2* mutant mice.²⁸ It is also possible that the decrease in HC number is due to a defect in differentiation, similar to that found in *Fgf20*^{-/-} cochleae.

Interestingly, both *Sall1*^{-/-} and *Sall1*^{+/+} cochleae contained numerous ectopic IHCs, found outside of the normal row of IHCs, a patterning defect that again is reminiscent of *Fgf20*^{-/-} and *Fgf20,Sox2* compound mutant phenotypes.^{9,13} Furthermore, *Sall1*^{+/+} cochleae also appeared to exhibit a delay in the apical progression of HC maturation, similar to *Fgf20*^{-/-} cochleae.⁹ The interaction between *Fgf20*, *Sox2*, and *Sall1* is a topic to explore in future studies.

The *Sall1*^{+/+} organ of Corti phenotype is consistently similar but more severe than that of *Sall1*^{-/-} cochleae. Since the *Sall1* truncated protein acts as a dominant negative on all members of the *Sall* family,^{47,49} this suggests that *Sall2* and/or *Sall3* have similar roles as *Sall1* in regulating cochlea development. Based on these results, we conclude that the decreased expression of *Sall1* and *Sall3* likely contributes to the OHC number and IHC patterning defects found in *Fgf20*^{-/-} cochleae.

Conclusions

The *Fgf20*^{-/-} cochlea phenotype includes loss of two-thirds of OHCs and outer supporting cells, abnormal patterning of the remaining HCs and SCs, shorter cochlea length, premature onset of differentiation, and delayed apical progression of differentiation and maturation. Here, we did not identify one single gene that can account for the majority of the *Fgf20*^{-/-} phenotype. However, we identified many FGF20-regulated genes that may contribute to parts of the phenotype. For instance, *Hey1*, *Hey2*, and possibly *Heyl* may account for the premature onset of differentiation phenotype; *Sall1*, *Sall3*, and *Fat3* may account for the OHC differentiation, patterning, and delay in maturation phenotypes; and cell cycle regulators such as *Cdc20* may account for the progenitor proliferation phenotypes in *Fgf20*, *Fgf9* and *Fgf20*, *Sox2* compound mutants. We conclude that FGF20 is likely not a straightforward outer HC and SC differentiation signal. Rather, the dramatic *Fgf20*^{-/-} phenotype may be the result of disruptions to a combination of FGF20-regulated processes, including prosensory progenitor proliferation, differentiation, maturation, and timing of differentiation. Given the complexity of OC development, we hypothesize that small disturbances to such processes can lead to much larger defects in overall development.

EXPERIMENTAL PROCEDURES

Mice

All studies performed were in accordance with the Institutional Animal Care and Use Committee at Washington University in St. Louis (protocol #20190110 and #20170258).

Mice were group housed with littermates, in breeding pairs, or in a breeding harem (two females to one male), with food and water provided ad libitum. Mice were of mixed sexes and maintained on a mixed C57BL/6J x 129X1/SvJ genetic background, except *Sall1*^{-/-} and *Sall1* mice, which were maintained on an ICR genetic background. The following mouse lines were used:

- *Fgf20*^{Cre}: knockin allele containing a sequence encoding a GFP-Cre fusion protein replacing exon 1 of *Fgf20*, resulting in a null mutation.¹⁰
- *Fgf20*^{βgal}: knockin allele containing a sequence encoding β-galactosidase (βgal) replacing exon 1 of *Fgf20*, resulting in a null mutation.⁹
- *ROSA*^{fsTRAP}: knockin allele containing a loxP-Stop-loxP sequence followed by a sequence encoding L10a-eGFP, targeted to the ubiquitously expressed *ROSA26* locus. Upon Cre-mediated recombination, the ribosomal protein L10a-eGFP is expressed.¹⁵
- *ROSA*^{mTmG}: knockin allele containing a sequence encoding a membrane-localized tdTomato (mT) flanked by loxP sequences, followed by a sequence encoding a membrane-localized eGFP (mG), targeted to the ubiquitously expressed *ROSA26* locus. In the absence of Cre-mediated recombination, mT is expressed; upon Cre-mediated recombination, mG is expressed instead.⁹⁸
- *Sall1*^{-/-}: knockin allele containing a sequence encoding GFP inserted in frame into exon 2 of *Sall1*, resulting in a null mutation.⁵⁰

- *Sall1- Zn2-10(Sall1)*: mutant allele expressing a truncated Sall1 protein designed to mimic a mutation that causes Townes-Brocks syndrome.⁴⁷
- *Cdc20^{fllox}*: allele containing loxP sequences flanking exon 2 of *Cdc20*; upon Cre-mediated recombination, results in a null allele.⁴²

Translating ribosome affinity purification (TRAP)

Affinity matrix preparation: for each immunoprecipitation (IP): 30 μ l of Streptavidin MyOne T1 Dynabeads (Invitrogen, 65602) were washed in 1x PBS using an end-over-end tube rotator and a magnet, and resuspended in 88 μ l of 1x PBS and conjugated to 12 μ l of 1 μ g/ μ l biotinylated protein L (Pierce 29997) in PBS for 35 min at room temperature (RT) with gentle end-over-end mixing on a tube rotator. Conjugated beads were then washed with 1x PBS + 3% IgG and protease-free BSA (Jackson ImmunoResearch, 001-000-162) x5, followed by three washes in low-salt buffer (20 mM HEPES KOH, pH 7.4, 10 mM MgCl₂, 150 mM KCl, 1% NP-40 [Sigma I8896-50ML], 0.5 mM DTT [Sigma, 646563], 100 μ g/ml cycloheximide [Sigma C4859-1ML]). Conjugated beads were then resuspended in low-salt buffer and mixed with 50 μ g each of anti-GFP antibodies Htz-GFP-19C8 and Htz-GFP-19F7 (Memorial Sloan-Kettering Monoclonal Antibody Facility) overnight at 4°C with gentle end-over-end mixing to make the affinity matrix. Immediately before IP, the affinity matrix was washed in low-salt buffer x3.

Sample collection: E14.5 embryos were harvested, on ice, from a mating producing a 1:1 ratio of *Fgf20^{Cre/+};ROSA^{fsTRAP/+}* and *Fgf20^{Cre/βgal};ROSA^{fsTRAP/+}* progeny. Embryos were staged based on vaginal plug (E0.5 at noon on the day plug is found) and on interdigital webbing. Embryos with too much or too little interdigital webbing were not harvested. Embryos were genotyped by LacZ staining to look for *Fgf20^{βgal}* expression in back skin hair follicles (back skin from embryos were incubated in 2 mM MgCl₂, 5 mM K3, 5 mM K4, 0.02% NP-40, and 1 mg/ml X-gal in N,N-dimethylformamide in 1x PBS for 30 min at 37°C, protected from light). Ventral otocysts from the embryos were dissected out in dissection buffer (1x HBSS, 2.5 mM HEPES-KOH, pH 7.4, 35 mM glucose, 4 mM NaHCO₃, 100 μ g/ml cycloheximide), separated from the dorsal otocyst (vestibule) without removal of the otic capsule, and pooled together by genotype. Each sample contained pooled ventral otocysts from 3-7 embryos. Pooled ventral otocysts were homogenized in lysis buffer (20 mM HEPES KOH, pH 7.4, 150 mM KCl, 10 mM MgCl₂, EDTA-free protease inhibitors (Roche, 04693159001), 0.5 mM DTT, 100 μ g/ml cycloheximide, 10 μ l/ml rRNasin (Promega N2515), 10 μ l/ml Superasin (Applied Biosystems, AM2696) using a pre-chilled Kontes homogenizer (Kontes, 885512-0020). To remove the nuclear fraction, homogenized samples were centrifuged for 10 min at 2000 g, 4°C. The supernatant (S2) was mixed with 1/8 volume of 10% NP-40 and 300 mM DHPC (reconstituted in lysis buffer; Avanti Polar Lipids 850306P) and incubated for 10 min on ice. To remove the mitochondrial fraction, samples were then centrifuged for 15 min at 20,000 g, 4°C. 60 μ l of the supernatant (S20) was saved as the pre-IP (pre-TRAP) control. The pre-TRAP S20 samples were incubated at 4°C until the RNA purification step, which was performed in conjunction with TRAP samples. The rest of the S20 was used for IP.

Immunoprecipitation: S20 was mixed with the affinity matrix for 24 hours at 4°C with end-over-end mixing. The mixture (TRAP sample) was washed in high-salt buffer (20 mM HEPES KOH, pH 7.4, 10 mM MgCl₂, 350 mM KCl, 1% NP-40, 0.5 mM DTT, 100 µg/ml cycloheximide, 1 µl/ml rRNasin, 1 µl/ml Supersasin) for 2 min at RT, x4.

RNA purification: the Arcturus Picopure RNA Isolation Kit (Thermo Fisher, 12204-01) was used to isolate RNA from pre-TRAP and TRAP samples according to manufacturer's instructions. RNA was eluted in 13 µl of elution buffer. Ventral otocysts from 3-7 embryos ranged between 4-20 ng of TRAP RNA. RNA samples were stored at -80°C until use in downstream applications.

Quantitative RT-PCR

cDNA was synthesized from pre-TRAP and TRAP RNA using the iScript Select cDNA Synthesis Kit (Bio-Rad, #170-8841) and quantified using TaqMan Fast Advanced Master Mix (Life Technologies, 4444557) with TaqMan assay probes for *Twist2* and *Id2*. *Gapdh* was used as normalization control. Results were analyzed by the CT method (normalized to *Gapdh*, then normalized to pre-TRAP). Each sample represents TRAP RNA from one litter.

cDNA library preparation and sequencing

cDNA library preparation and sequencing were performed at the Genome Technology Access Center (GTAC) at Washington University (gtac.wustl.edu). RNA samples were analyzed on an Agilent 2100 Bioanalyzer; all sequenced RNA samples had an RNA Integrity Number (RIN) of ≥ 8.8. Clontech SMARTer Ultra Low Input RNA for Illumina Sequencing - HV kit (Takara Bio, 634828), which utilizes both oligo(dT) and random priming, was used for cDNA library preparation and amplification. The TRAPseq results presented are from two sequencing experiments. cDNA library preparation was performed independently in the two experiments. In both experiments, 8 TRAP samples (4 *Fgf20*^{-/+} and 4 *Fgf20*^{-/-}) and 4 pre-TRAP samples (2 *Fgf20*^{-/+} and 2 *Fgf20*^{-/-}) were sequenced on one Illumina HiSeq 3000 lane, with single reads, 1 × 50 bps. 24 samples were sequenced in total between the two experiments (12 samples multiplexed per lane per experiment). Sequencing produced between 22 and 38 million reads per sample.

Bioinformatic analysis

Basecalling was performed with Illumina RealTimeAnalysis software. The resulting bcl files were demultiplexed with Illumina's bclToFastq2. Both steps were performed by GTAC.

Alignment: Reads were mapped to GRCm38.p5 (Ensemble, GCA_000001635.7) using STAR aligner,⁹⁹ with the GRCm38.91 annotation file (Ensembl).¹⁰⁰ Default parameters were used, except for the following: multi-sample 2-pass, with default settings on first pass and sjdbFileChrStartEnd (for novel splice junctions), ScoreMinOverLread=0.4, MatchNminOverLread=0.4, MismatchNmax=5 on second pass (these parameters gave the most consistent unmapped reads % across all 24 TRAPseq samples). 95-99.5% of reads were mapped per sample.

Counting and DEG analysis: Analyses were performed in R using packages from Bioconductor (bioconductor.org). BAM files were indexed and sorted using Rsamtools.¹⁰¹ Gene models were defined using the GRCm38.91 annotation file (Ensembl) with GenomicFeatures.¹⁰² Reads were counted using the SummarizeOverlaps method (mode = Union) from the package GenomicAlignments.¹⁰² Genes were filtered out from downstream analysis if less than 8 of 24 samples had 25 or more reads. PC analysis showed separation between the 8 pre-TRAP samples and 16 TRAP samples along PC1, and also separation between sequencing experiment 1 and experiment 2 along PC2. Removal of Unwanted Variation from RNA-Seq Data (RUVSeq) was used to correct for this batch effect (RUVs function, $k = 1$).¹⁰³ DESeq2 with RUVs correction factors was used for DEG analysis, with $\alpha = 0.1$ and Benjamini-Hochberg multiple-comparisons correction.¹⁹

Pathway analysis: gene ontology (GO) analysis was performed using the Bioconductor package topGO with the following parameters: nodeSize = 10; ontology = biological processes (BP); algorithm = elim; statistic = fisher's exact test.¹⁰⁴ Protein-protein interaction network analysis was performed using STRING version 11.0 with the following parameters: active interaction sources include textmining, experiments, databases, co-expression, neighborhood, gene fusion, co-occurrence; minimum required interaction score = high confidence (0.700).^{37,38}

Sample preparation and sectioning for histology and in situ hybridization

For whole mount cochleae, inner ears were dissected out of P0 pups and fixed in 4% PFA in PBS overnight at 4°C with gentle agitation. Samples were then washed x3 in PBS. Cochleae were dissected away from the vestibule, otic capsule, and periotic mesenchyme with Dumont #55 Forceps (Roboz, RS-5010). The roof of the cochlear duct was opened by dissecting away the stria vascularis and Reissner's membrane; tectorial membrane was removed to expose hair and supporting cells.

For sectioning, heads from E14.5 embryos were fixed in 4% PFA in PBS overnight at 4°C with gentle agitation. Samples were then washed x3 in PBS and cryoprotected in 15% sucrose in PBS overnight and then in 30% sucrose in PBS overnight. Samples were embedded in Tissue-Tek O.C.T. compound (VWR International, 4583) and frozen on dry ice. Serial horizontal sections through base of the head were cut at 12 μm with a cryostat, dried at room temperature, and stored at -80°C until use.

RNA in situ hybridization

Probe preparation: plasmids containing the following mouse cDNA inserts were used to make digoxigenin-labeled riboprobes, and were linearized and transcribed with the indicated restriction enzyme (New England Biolabs) and RNA polymerase (New England Biolabs) according to the manufacturers' instructions, with DIG RNA Labeling Mix (Sigma-Aldrich, 11277073910). Probes were treated with RNase-free DNase I (Sigma-Aldrich, 04716728001) for 15 min at 37°C, then hydrolyzed in 40 mM NaHCO₃, 60 mM Na₂CO₃ at 60°C for 5-30 min, to make 300-400 bp probes. *Dusp6* (412 bp, Acc65I, T7, gift of S. Mansour),⁷⁶ *Etv1* (2500 bp, SpeI, T7, addgene #16282, gift of S.-H. Huh), *Spry1* (1500 bp, EcoRI, T7),³³ *Spry4* (900 bp, EcoRI, T7),³³ *Tectb* (2746 bp, EcoRI, T7, gift of D. Wu),⁵⁶

Tecta (4382 bp, NotI, T7, gift of D. Wu),⁵⁶ *Epyc* (1522 bp, EcoRI, T7, Image clone 4037028), *Heyl* (1895, BamHI, T7, Image clone 40142873), *Gata2* (700 bp, BamHI, T3, gift of D. Wu), *Meis2* (~5000 bp, EcoRI, T3, gift of Y. Yang), *Lmx1a* (600 bp, SphI, Sp6, gift of D. Wu),¹⁰⁵ and *Bmp4* (AccI, T7).¹⁰⁶

Sall1 probe was made from *pBluescript KS (+)-Sall1* cDNA clone (GenBank accession no. [NM_001371070.1](#) nucleotides 856 to 1283 inserted into the EcoRV site), which was linearized with HindIII and transcribed with T7. *Sall2* probe was made from *pBluescript II KS (+)-Sall2* cDNA clone (GenBank accession no. [NM_015772](#) nucleotides 687 to 1113 inserted into the PstI/EcoRI site), which was linearized with EcoRI and transcribed with T7. *Sall3* probe was made from *pBluescript II KS (+)-Sall3* cDNA clone (GenBank accession no. [NM_001369133](#) nucleotides 575 to 1124 inserted into the HincII site) which was linearized with XbaI and transcribed with T3).

Smpx probe was made from PCR product containing T7 promoter sequence (gift of J. Bok),⁶⁴ and transcribed with T7. *Fat3* probe was made by PCR amplification of a plasmid containing 945 bp sequence of *Fat3* cDNA (gift of L. Goodrich) using primers F: 5'-ACAGCTCGCATCAGCTTCGTGT-3' and R (containing T7 promoter sequence): 5'-GGATCCTAATACGACTCACTATAGGGAGTGCTTTGCAGGGTTCTCAGGC-3', and transcribed with T7. *Cdc20* probe was made by PCR amplification of mouse tail genomic DNA using primers F: 5'-GTTCGGGAGAGCTGAGTACG-3' and R (containing T7 promoter sequence): 5'-GGATCCTAATACGACTCACTATAGGGAGGCTGTGTGATCTGTTGGCG-3', and transcribed with T7.

Frozen section in situ hybridization: frozen slides were warmed for 20 min at room temperature and then 5 min at 50°C on a slide warmer. Sections were fixed in 4% PFA in PBS for 20 min at room temperature, washed x2 in PBS and treated with pre-warmed 10 µg/ml Proteinase K (Sigma-Aldrich, 03115828001) in PBS for 1 min (E12.5 samples) or 7 min (E14.5 samples) at 37°C. Sections were then fixed in 4% PFA in PBS for 15 min at room temperature, washed x2 in PBS, acetylated in 0.25% acetic anhydride in 0.1M Triethanolamine, pH 8.0, for 10 min, and washed again in PBS. Sections were then placed in pre-warmed hybridization buffer (50% formamide, 5x SSC buffer, 5 mM EDTA, 50 µg/ml yeast tRNA) for 3 h at 60–65°C in humidified chamber for prehybridization. Sections were then hybridized in 10 µg/ml probe/hybridization buffer overnight (12–16 h) at 60–65°C. The next day, sections were washed in 1x SSC for 10 min at 60°C, followed by 1.5x SSC for 10 min at 60°C, 2x SSC for 20 min at 37°C x2, and 0.2x SSC for 30 min at 60°C x2. Sections were then washed in KTBT (0.1 M Tris, pH 7.5, 0.15 M NaCl, 5 mM KCl, 0.1% Triton X-100) at room temperature and blocked in KTBT + 20% sheep serum + 2% Blocking Reagent (Sigma-Aldrich, 11096176001) for 4 h. Blocking Reagent was dissolved in 100 mM Maleic acid, 150 mM NaCl, pH 7.5. Sections were then incubated in sheep anti-Digoxigenin-AP, Fab fragments (1:1000, Sigma-Aldrich, 11093274910) in KTBT + 20% sheep serum + 2% Blocking Reagent overnight at 4°C. Sections were then washed x3 in KTBT for 30 min at room temperature, and then washed x2 in NTMT (0.1 M Tris, pH 9.5, 0.1 M NaCl, 50 mM MgCl₂, 0.1% Tween 20) for 15 min. Sections were next incubated in NTMT + 1:200 NBT/BCIP Stock Solution (Sigma-Aldrich, 11681451001) in the dark at

room temperature until color appeared. Sections were then washed in PBS, post-fixed in 4% PFA in PBS for 15 min and washed x2 in PBS. Finally, sections were dehydrated in 30% and then 70% methanol, 5 min each, followed by 100% methanol for 15 min. Sections were then rehydrated in 70% and 30% methanol and then PBS, 5 min each, and mounted in 95% glycerol.

Immunofluorescence

Whole mount: cochleae were incubated in PBS + 0.5% Tween-20 (PBSTw) for 1 h to permeabilize. Cochleae were then blocked using PBSTw + 5% donkey serum for 1 h and then incubated in PBSTw + 1% donkey serum with the primary antibody overnight at 4°C. Cochleae were then washed x3 in PBS and incubated in PBS + 1% Tween-20 with the secondary antibody. After wash in PBS x3, cochleae were mounted in 95% glycerol or VectaShield antifade mounting medium with DAPI (Vector Labs, H-1200) with the sensory epithelium facing up.

Frozen slides were warmed for 30 min at room temperature and washed in PBS before incubating in PBS + 0.5% Triton X-100 (PBST) for 1 h to permeabilize the tissue. Sections were then blocked using in PBST + 5% donkey serum for 1 h and then incubated in PBST + 1% donkey serum with the primary antibody overnight at 4°C in a humidified chamber. Sections were then washed x3 in PBS and incubated in PBS + 1% Triton X-100 with the secondary antibody. After wash in PBS x3, slides were mounted in VectaShield antifade mounting medium with DAPI.

The following compounds and antibodies were used:

- Alexa Fluor 488-conjugated Phalloidin (1:50, Invitrogen, A12379)
- Rabbit anti-P75NTR (1:300, EMD Millipore, AB1554)
- Alexa Fluor 555 goat anti-rabbit IgG (1:500, Invitrogen, A21428)

Imaging

Light microscopy: slides were scanned using a Hamamatsu NanoZoomer slide scanning system with a 20x objective. Images were then processed with the NanoZoomer Digital Pathology (NDP.view2) software. 3D specimens were imaged using an Olympus SZXZ110 stereo microscope equipped with an Olympus DP70 camera.

Fluorescent microscopy was performed using a Zeiss LSM 700 confocal or Zeiss Axio Imager Z1 with Apotome 2, with z-stack step-size determined based on objective lens type (10x or 20x), as recommended by the ZEN software (around 1 μ m). Fluorescent images shown are maximum projections. Images were processed with ImageJ (imagej.nih.gov).

Image analysis and quantification

Measurements and cell quantification (using the Cell Counter plugin by Kurt De Vos) were performed using Fiji.¹⁰⁷ Total cochlear duct length was defined as the length from the very base of the cochlea to the very tip of the apex, along the tunnel of Corti, measured on whole-mount cochlea. Hair cells and stereocilia bundles were identified via Phalloidin, which binds

to F-actin.¹⁰⁸ Inner pillar cells were labeled via P75NTR.¹⁰⁹ Inner hair cells (IHCs) were differentiated from outer hair cells (OHCs) based on their neural/abneural location, respectively, relative to P75NTR-expressing inner pillar cells. For total cell counts, IHCs and OHCs were counted along the entire length of the cochlea.

Statistical analysis and plotting

All figures were made in Canvas X (ACD systems). RNA sequencing data analysis and plotting were performed using R (r-project.org) in R studio (rstudio.com) PCA graphs were made using the plotPCA function from the Bioconductor package RUVSeq; volcano plots were made using modified code from Stephen Turner (gist.github.com/stephenturner). See Bioinformatic analysis section for more details on RNA sequencing data analysis. All other data analysis and plotting were performed using Python (python.org) in Jupyter Notebook (jupyter.org) with the following libraries: Pandas (pandas.pydata.org), Seaborn (seaborn.pydata.org), NumPy (numpy.org) and SciPy (scipy.org). Plotting was performed using the Matplotlib library (matplotlib.org). Statistics (t-test, one-way ANOVA, and two-way ANOVA) were performed using the SciPy module Stats; Tukey's HSD was performed using the Statsmodels package (statsmodels.org). All comparisons of two means were performed using two-tailed, unpaired Student's t-test. For comparisons of more than two means, one-way ANOVA was used. For significant ANOVA results at $\alpha = 0.05$, Tukey's HSD was performed for post-hoc pair-wise analysis. In all cases, $p < 0.05$ was considered statistically significant. All statistical details can be found in the figures and figure legends. In all cases, each sample (each data point in graphs) represents one animal. Based on similar previous studies, a sample size of 3-5 was determined to be appropriate. Error bars represent mean \pm standard deviation. For qualitative comparisons (comparing expression via immunofluorescence or RNA in situ hybridization), at least three samples were examined per genotype. All images shown are representative. No data were excluded from analysis.

Supplementary Material

Refer to Web version on PubMed Central for supplementary material.

ACKNOWLEDGEMENTS

We thank J. Dougherty and his laboratory for their help with the TRAP technique, B. Zhang (Department of Developmental Biology), and T. Sinnwell and M. Heinz (Genome Technology Access Center in the Department of Genetics) for their help with RNA sequencing and analysis. We thank L. Robbins for generating the *Sall1*, *Sall2*, and *Sall3* plasmids used for making in situ probes. We also thank C. Ferguson for supplying us with *Cdc20^{fllox}* mice. This work was funded by the Department of Developmental Biology at Washington University, NIH/National Institute on Deafness and Other Communication Disorders grant DC017042 (DMO), the Washington University Institute of Clinical and Translational Sciences which is, in part, supported by the NIH/National Center for Advancing Translational Sciences, CTSA grant UL1TR002345 (JIT471 to DMO), March of Dimes grant 6-FY13-127 (MR), and the Rare Disease Foundation/BC Children's Hospital Foundation. GTAC is partially supported by NCI Cancer Center Support Grant P30 CA91842 to the Siteman Cancer Center and by ICTS/CTSA Grant UL1TR000448 from the National Center for Research Resources (NCCR). HOPE Center Alafi Neuroimaging Laboratory is supported by NCCR grant 1S10RR027552, the Auditory and Vestibular Microscopy and Digital Imaging Core is supported by NIH grant P30 DC004665. The authors have no conflicts of interest to disclose.

Data availability:

The data discussed in this publication have been deposited in NCBI's Gene Expression Omnibus and are accessible through GEO Series accession number GSE148380 (<https://www.ncbi.nlm.nih.gov/geo/query/acc.cgi?acc=GSE148380>).¹¹⁰

List of abbreviations:

DEG	differentially expressed gene
GER	greater epithelial ridge
GO	gene ontology
HC	hair cell
IHC	inner hair cell
ISH	in situ hybridization
IP	immunoprecipitation
KO	Kölliker's organ
LER	lesser epithelial ridge
OC	organ of Corti
OHC	outer hair cell
OS	outer sulcus
padj	adjusted p-value
PCA	principal component analysis
PD	prosensory domain
SC	supporting cell
TBS	Townes-Brocks syndrome
TRAP	translating ribosome affinity purification
TRAPseq	TRAP combined with next generation RNA sequencing

REFERENCES

1. Allen SB, Goldman J. Syndromic Sensorineural Hearing Loss (SSHL) In: StatPearls. StatPearls Publishing; 2019 Accessed April 8, 2020 <http://www.ncbi.nlm.nih.gov/books/NBK526088/>
2. Basch ML, Brown RM, Jen H-I, Groves AK. Where hearing starts: the development of the mammalian cochlea. *J Anat.* 2016;228(2):233–254. doi:10.1111/joa.12314 [PubMed: 26052920]
3. Bowl MR, Brown SDM. Genetic landscape of auditory dysfunction. *Hum Mol Genet.* 2018;27(R2):R130–R135. doi:10.1093/hmg/ddy158 [PubMed: 29726933]

4. Wu DK, Kelley MW. Molecular Mechanisms of Inner Ear Development. *Cold Spring Harb Perspect Biol.* 2012;4(8):a008409. doi:10.1101/cshperspect.a008409 [PubMed: 22855724]
5. Wong ACY, Ryan AF. Mechanisms of sensorineural cell damage, death and survival in the cochlea. *Front Aging Neurosci.* 2015;7:58. doi:10.3389/fnagi.2015.00058 [PubMed: 25954196]
6. Yamasoba T, Lin FR, Someya S, Kashio A, Sakamoto T, Kondo K. Current concepts in age-related hearing loss: epidemiology and mechanistic pathways. *Hear Res.* 2013;303:30–38. doi:10.1016/j.heares.2013.01.021 [PubMed: 23422312]
7. Corwin JT, Warchol ME. Auditory hair cells: structure, function, development, and regeneration. *Annu Rev Neurosci.* 1991;14:301–333. doi:10.1146/annurev.ne.14.030191.001505 [PubMed: 2031573]
8. Hayashi T, Ray CA, Bermingham-McDonogh O. Fgf20 Is Required for Sensory Epithelial Specification in the Developing Cochlea. *J Neurosci.* 2008;28(23):5991–5999. doi:10.1523/JNEUROSCI.1690-08.2008 [PubMed: 18524904]
9. Huh S-H, Jones J, Warchol ME, Ornitz DM. Differentiation of the Lateral Compartment of the Cochlea Requires a Temporally Restricted FGF20 Signal. *PLOS Biol.* 2012;10(1):e1001231. doi:10.1371/journal.pbio.1001231 [PubMed: 22235191]
10. Huh S-H, Warchol ME, Ornitz DM. Cochlear progenitor number is controlled through mesenchymal FGF receptor signaling. *eLife.* 2015;4:e05921. doi:10.7554/eLife.05921
11. Ono K, Kita T, Sato S, et al. FGFR1-Frs2/3 Signalling Maintains Sensory Progenitors during Inner Ear Hair Cell Formation. *PLOS Genet.* 2014;10(1):e1004118. doi:10.1371/journal.pgen.1004118 [PubMed: 24465223]
12. Pirvola U, Ylikoski J, Trokovic R, Hébert JM, McConnell SK, Partanen J. FGFR1 is required for the development of the auditory sensory epithelium. *Neuron.* 2002;35(4):671–680. doi:10.1016/s0896-6273(02)00824-3 [PubMed: 12194867]
13. Yang LM, Cheah KSE, Huh S-H, Ornitz DM. Sox2 and FGF20 interact to regulate organ of Corti hair cell and supporting cell development in a spatially-graded manner. *PLOS Genet.* 2019;15(7):e1008254. doi:10.1371/journal.pgen.1008254 [PubMed: 31276493]
14. Heiman M, Schaefer A, Gong S, et al. A translational profiling approach for the molecular characterization of CNS cell types. *Cell.* 2008;135(4):738–748. doi:10.1016/j.cell.2008.10.028 [PubMed: 19013281]
15. Zhou P, Zhang Y, Ma Q, et al. Interrogating translational efficiency and lineage-specific transcriptomes using ribosome affinity purification. *Proc Natl Acad Sci U S A.* 2013;110(38):15395–15400. doi:10.1073/pnas.1304124110 [PubMed: 24003143]
16. Kohlhasse J, Wischermann A, Reichenbach H, Froster U, Engel W. Mutations in the SALL1 putative transcription factor gene cause Townes-Brocks syndrome. *Nat Genet.* 1998;18(1):81–83. doi:10.1038/ng0198-81 [PubMed: 9425907]
17. Rossmiller DR, Pasic TR. Hearing loss in Townes-Brocks syndrome. *Otolaryngol Head Neck Surg.* 1994;111(3 Pt 1):175–180. doi:10.1177/01945998941113P103 [PubMed: 8084622]
18. Jones JM, Montcouquiol M, Dabdoub A, Woods C, Kelley MW. Inhibitors of differentiation and DNA binding (Ids) regulate Math1 and hair cell formation during the development of the organ of Corti. *J Neurosci.* 2006;26(2):550–558. doi:10.1523/JNEUROSCI.3859-05.2006 [PubMed: 16407553]
19. Love MI, Huber W, Anders S. Moderated estimation of fold change and dispersion for RNA-seq data with DESeq2. *Genome Biol.* 2014;15:550. doi:10.1186/s13059-014-0550-8 [PubMed: 25516281]
20. Zhu H, Mitsuhashi N, Klein A, et al. The role of the hyaluronan receptor CD44 in mesenchymal stem cell migration in the extracellular matrix. *Stem Cells.* 2006;24(4):928–935. doi:10.1634/stemcells.2005-0186 [PubMed: 16306150]
21. Cooley MA, Kern CB, Fresco VM, et al. Fibulin-1 is required for morphogenesis of neural crest-derived structures. *Dev Biol.* 2008;319(2):336–345. doi:10.1016/j.ydbio.2008.04.029 [PubMed: 18538758]
22. Karnik SK, Brooke BS, Bayes-Genis A, et al. A critical role for elastin signaling in vascular morphogenesis and disease. *Development.* 2003;130(2):411–423. doi:10.1242/dev.00223 [PubMed: 12466207]

23. Fujita T, Azuma Y, Fukuyama R, et al. Runx2 induces osteoblast and chondrocyte differentiation and enhances their migration by coupling with PI3K-Akt signaling. *J Cell Biol.* 2004;166(1):85–95. doi:10.1083/jcb.200401138 [PubMed: 15226309]
24. Pei M, Luo J, Chen Q. Enhancing and maintaining chondrogenesis of synovial fibroblasts by cartilage extracellular matrix protein matrilins. *Osteoarthritis Cartilage.* 2008;16(9):1110–1117. doi:10.1016/j.joca.2007.12.011 [PubMed: 18282772]
25. Lilleväli K, Matilainen T, Karis A, Salminen M. Partially overlapping expression of Gata2 and Gata3 during inner ear development. *Dev Dyn.* 2004;231(4):775–781. doi:10.1002/dvdy.20185 [PubMed: 15499560]
26. Ohyama T, Basch ML, Mishina Y, Lyons KM, Segil N, Groves AK. BMP Signaling Is Necessary for Patterning the Sensory and Nonsensory Regions of the Developing Mammalian Cochlea. *J Neurosci.* 2010;30(45):15044–15051. doi:10.1523/JNEUROSCI.3547-10.2010 [PubMed: 21068310]
27. Basch ML, Ohyama T, Segil N, Groves AK. Canonical Notch Signaling Is Not Necessary for Prosensory Induction in the Mouse Cochlea: Insights from a Conditional Mutant of RBPj. *J Neurosci.* 2011;31(22):8046–8058. doi:10.1523/JNEUROSCI.6671-10.2011 [PubMed: 21632926]
28. Kiernan AE, Pelling AL, Leung KKH, et al. Sox2 is required for sensory organ development in the mammalian inner ear. *Nature.* 2005;434(7036):1031–1035. doi:10.1038/nature03487 [PubMed: 15846349]
29. Luo X, Deng M, Xie X, et al. GATA3 controls the specification of prosensory domain and neuronal survival in the mouse cochlea. *Hum Mol Genet.* 2013;22(18):3609–3623. doi:10.1093/hmg/ddt212 [PubMed: 23666531]
30. Woods C, Montcouquiol M, Kelley MW. Math1 regulates development of the sensory epithelium in the mammalian cochlea. *Nat Neurosci.* 2004;7(12):1310–1318. doi:10.1038/nn1349 [PubMed: 15543141]
31. Locher H, de Groot JCMJ, van Iperen L, Huisman MA, Frijns JHM, de S Lopes SMC. Distribution and Development of Peripheral Glial Cells in the Human Fetal Cochlea. *PLOS ONE.* 2014;9(1):e88066. doi:10.1371/journal.pone.0088066 [PubMed: 24498246]
32. Puligilla C, Dabdoub A, Brenowitz SD, Kelley MW. Sox2 Induces Neuronal Formation in the Developing Mammalian Cochlea. *J Neurosci.* 2010;30(2):714–722. doi:10.1523/JNEUROSCI.3852-09.2010 [PubMed: 20071536]
33. Minowada G, Jarvis LA, Chi CL, et al. Vertebrate Sprouty genes are induced by FGF signaling and can cause chondrodysplasia when overexpressed. *Development.* 1999;126(20):4465–4475. [PubMed: 10498682]
34. Münchberg SR, Steinbeisser H. The Xenopus Ets transcription factor XER81 is a target of the FGF signaling pathway. *Mech Dev.* 1999;80(1):53–65. doi:10.1016/s0925-4773(98)00193-2 [PubMed: 10096063]
35. Willardsen M, Hutcheson DA, Moore KB, Vetter ML. The ETS transcription factor Etv1 mediates FGF signaling to initiate proneural gene expression during *Xenopus laevis* retinal development. *Mech Dev.* 2014;131:57–67. doi:10.1016/j.mod.2013.10.003 [PubMed: 24219979]
36. Yang LM, Huh S-H, Ornitz DM. FGF20-Expressing, Wnt-Responsive Olfactory Epithelial Progenitors Regulate Underlying Turbinate Growth to Optimize Surface Area. *Dev Cell.* 2018;46(5):564–580.e5. doi:10.1016/j.devcel.2018.07.010 [PubMed: 30100263]
37. Snel B, Lehmann G, Bork P, Huynen MA. STRING: a web-server to retrieve and display the repeatedly occurring neighbourhood of a gene. *Nucleic Acids Res.* 2000;28(18):3442–3444. doi:10.1093/nar/28.18.3442 [PubMed: 10982861]
38. Szklarczyk D, Gable AL, Lyon D, et al. STRING v11: protein-protein association networks with increased coverage, supporting functional discovery in genome-wide experimental datasets. *Nucleic Acids Res.* 2019;47(D1):D607–D613. doi:10.1093/nar/gky1131 [PubMed: 30476243]
39. Yang Y, Kim AH, Yamada T, et al. A Cdc20-APC ubiquitin signaling pathway regulates presynaptic differentiation. *Science.* 2009;326(5952):575–578. doi:10.1126/science.1177087 [PubMed: 19900895]
40. Chen P, Segil N. p27(Kip1) links cell proliferation to morphogenesis in the developing organ of Corti. *Development.* 1999;126(8):1581–1590. [PubMed: 10079221]

41. Lee Y-S, Liu F, Segil N. A morphogenetic wave of p27Kip1 transcription directs cell cycle exit during organ of Corti development. *Development*. 2006;133(15):2817–2826. doi:10.1242/dev.02453 [PubMed: 16790479]
42. Manchado E, Guillamot M, de Cárcer G, et al. Targeting mitotic exit leads to tumor regression in vivo: Modulation by Cdk1, Mastl, and the PP2A/B55 α , δ phosphatase. *Cancer Cell*. 2010;18(6):641–654. doi:10.1016/j.ccr.2010.10.028 [PubMed: 21156286]
43. Nishinakamura R, Matsumoto Y, Nakao K, et al. Murine homolog of SALL1 is essential for ureteric bud invasion in kidney development. *Development*. 2001;128(16):3105–3115. [PubMed: 11688560]
44. Ott T, Kaestner KH, Monaghan AP, Schütz G. The mouse homolog of the region specific homeotic gene spalt of *Drosophila* is expressed in the developing nervous system and in mesoderm-derived structures. *Mech Dev*. 1996;56(1):117–128. doi:10.1016/0925-4773(96)00516-3 [PubMed: 8798152]
45. Ott T, Parrish M, Bond K, Schwaeger-Nickolenko A, Monaghan AP. A new member of the spalt like zinc finger protein family, Msal-3, is expressed in the CNS and sites of epithelial/mesenchymal interaction. *Mech Dev*. 2001;101(1–2):203–207. doi:10.1016/S0925-4773(00)00552-9 [PubMed: 11231076]
46. Parrish M, Ott T, Lance-Jones C, Schuetz G, Schwaeger-Nickolenko A, Monaghan AP. Loss of the Sall3 Gene Leads to Palate Deficiency, Abnormalities in Cranial Nerves, and Perinatal Lethality. *Mol Cell Biol*. 2004;24(16):7102–7112. doi:10.1128/MCB.24.16.7102-7112.2004 [PubMed: 15282310]
47. Kiefer SM, Ohlemiller KK, Yang J, McDill BW, Kohlhasse J, Rauchman M. Expression of a truncated Sall1 transcriptional repressor is responsible for Townes–Brocks syndrome birth defects. *Hum Mol Genet*. 2003;12(17):2221–2227. doi:10.1093/hmg/ddg233 [PubMed: 12915476]
48. Kiefer SM, McDill BW, Yang J, Rauchman M. Murine Sall1 represses transcription by recruiting a histone deacetylase complex. *J Biol Chem*. 2002;277(17):14869–14876. doi:10.1074/jbc.M200052200 [PubMed: 11836251]
49. Kiefer SM, Robbins L, Barina A, Zhang Z, Rauchman M. SALL1 truncated protein expression in Townes-Brocks syndrome leads to ectopic expression of downstream genes. *Hum Mutat*. 2008;29(9):1133–1140. doi:10.1002/humu.20759 [PubMed: 18470945]
50. Takasato M, Osafune K, Matsumoto Y, et al. Identification of kidney mesenchymal genes by a combination of microarray analysis and Sall1-GFP knockin mice. *Mech Dev*. 2004;121(6):547–557. doi:10.1016/j.mod.2004.04.007 [PubMed: 15172686]
51. Paralkar VR, Taborda CC, Huang P, et al. Unlinking an lncRNA from Its Associated cis Element. *Mol Cell*. 2016;62(1):104–110. doi:10.1016/j.molcel.2016.02.029 [PubMed: 27041223]
52. Haque K, Pandey AK, Zheng H-W, Riazuddin S, Sha S-H, Puligilla C. MEKK4 Signaling Regulates Sensory Cell Development and Function in the Mouse Inner Ear. *J Neurosci*. 2016;36(4):1347–1361. doi:10.1523/JNEUROSCI.1853-15.2016 [PubMed: 26818521]
53. Saburi S, Hester I, Goodrich L, McNeill H. Functional interactions between Fat family cadherins in tissue morphogenesis and planar polarity. *Development*. 2012;139(10):1806–1820. doi:10.1242/dev.077461 [PubMed: 22510986]
54. Buniello A, Hardisty-Hughes RE, Pass JC, Bober E, Smith RJ, Steel KP. Headbobber: a combined morphogenetic and cochleolaccular mouse model to study 10qter deletions in human deafness. *PLOS One*. 2013;8(2):e56274. doi:10.1371/journal.pone.0056274 [PubMed: 23457544]
55. Somma G, Alger HM, McGuire RM, et al. Head bobber: an insertional mutation causes inner ear defects, hyperactive circling, and deafness. *J Assoc Res Otolaryngol*. 2012;13(3):335–349. doi:10.1007/s10162-012-0316-5 [PubMed: 22383091]
56. Rau A, Legan PK, Richardson GP. Tectorin mRNA expression is spatially and temporally restricted during mouse inner ear development. *J Comp Neurol*. 1999;405(2):271–280. doi:10.1002/(SICI)1096-9861(19990308)405:2<271::AID-CNE10>3.0.CO;2-2 [PubMed: 10023815]
57. Russell IJ, Legan PK, Lukashkina VA, Lukashkin AN, Goodyear RJ, Richardson GP. Sharpened cochlear tuning in a mouse with a genetically modified tectorial membrane. *Nat Neurosci*. 2007;10(2):215–223. doi:10.1038/nn1828 [PubMed: 17220887]

58. Forrest D, Erway LC, Ng L, Altschuler R, Curran T. Thyroid hormone receptor beta is essential for development of auditory function. *Nat Genet.* 1996;13(3):354–357. doi:10.1038/ng0796-354 [PubMed: 8673137]
59. Griffith AJ, Szymko YM, Kaneshige M, et al. Knock-in mouse model for resistance to thyroid hormone (RTH): an RTH mutation in the thyroid hormone receptor beta gene disrupts cochlear morphogenesis. *J Assoc Res Otolaryngol.* 2002;3(3):279–288. doi:10.1007/s101620010092 [PubMed: 12382103]
60. Kaukua N, Shahidi MK, Konstantinidou C, et al. Glial origin of mesenchymal stem cells in a tooth model system. *Nature.* 2014;513(7519):551–554. doi:10.1038/nature13536 [PubMed: 25079316]
61. Ng L, Cordas E, Wu X, Vella KR, Hollenberg AN, Forrest D. Age-related hearing loss and degeneration of cochlear hair cells in mice lacking thyroid hormone receptor β 1. *Endocrinology.* 2015;156(10):3853–3865. doi:10.1210/en.2015-1468 [PubMed: 26241124]
62. Sharlin DS, Visser TJ, Forrest D. Developmental and cell-specific expression of thyroid hormone transporters in the mouse cochlea. *Endocrinology.* 2011;152(12):5053–5064. doi:10.1210/en.2011-1372 [PubMed: 21878515]
63. Yamamoto N, Okano T, Ma X, Adelstein RS, Kelley MW. Myosin II regulates extension, growth and patterning in the mammalian cochlear duct. *Development.* 2009;136(12):1977–1986. doi:10.1242/dev.030718 [PubMed: 19439495]
64. Yoon H, Lee DJ, Kim MH, Bok J. Identification of genes concordantly expressed with Atoh1 during inner ear development. *Anat Cell Biol.* 2011;44(1):69–78. doi:10.5115/acb.2011.44.1.69 [PubMed: 21519551]
65. Abdelfatah N, Merner N, Houston J, et al. A Novel Deletion in SMPX Causes a Rare form of X-Linked Progressive Hearing Loss in Two Families Due to a Founder Effect. *Hum Mutat.* 2013;34(1):66–69. doi:10.1002/humu.22205 [PubMed: 22911656]
66. Huebner AK, Gandia M, Frommolt P, et al. Nonsense mutations in SMPX, encoding a protein responsive to physical force, result in X-chromosomal hearing loss. *Am J Hum Genet.* 2011;88(5):621–627. doi:10.1016/j.ajhg.2011.04.007 [PubMed: 21549336]
67. Schraders M, Haas SA, Weegerink NJD, et al. Next-generation sequencing identifies mutations of SMPX, which encodes the small muscle protein, X-linked, as a cause of progressive hearing impairment. *Am J Hum Genet.* 2011;88(5):628–634. doi:10.1016/j.ajhg.2011.04.012 [PubMed: 21549342]
68. Palmer S, Groves N, Schindeler A, et al. The Small Muscle-Specific Protein Csl Modifies Cell Shape and Promotes Myocyte Fusion in an Insulin-like Growth Factor 1-Dependent Manner. *J Cell Biol.* 2001;153(5):985–998. doi:10.1083/jcb.153.5.985 [PubMed: 11381084]
69. Hanada Y, Nakamura Y, Ishida Y, et al. Epiphycan is specifically expressed in cochlear supporting cells and is necessary for normal hearing. *Biochem Biophys Res Commun.* 2017;492(3):379–385. doi:10.1016/j.bbrc.2017.08.092 [PubMed: 28864419]
70. Benito-Gonzalez A, Doetzlhofer A. Hey1 and Hey2 Control the Spatial and Temporal Pattern of Mammalian Auditory Hair Cell Differentiation Downstream of Hedgehog Signaling. *J Neurosci.* 2014;34(38):12865–12876. doi:10.1523/JNEUROSCI.1494-14.2014 [PubMed: 25232121]
71. Hayashi T, Kokubo H, Hartman BH, Ray CA, Reh TA, Bermingham-McDonogh O. Hes1 and Hes2 may act as early effectors of Notch signaling in the developing cochlea. *Dev Biol.* 2008;316(1):87–99. doi:10.1016/j.ydbio.2008.01.006 [PubMed: 18291358]
72. Doetzlhofer A, Basch ML, Ohyama T, Gessler M, Groves AK, Segil N. Hey2 Regulation by FGF Provides a Notch-Independent Mechanism for Maintaining Pillar Cell Fate in the Organ of Corti. *Dev Cell.* 2009;16(1):58–69. doi:10.1016/j.devcel.2008.11.008 [PubMed: 19154718]
73. Tateya T, Imayoshi I, Tateya I, Ito J, Kageyama R. Cooperative functions of Hes/Hey genes in auditory hair cell and supporting cell development. *Dev Biol.* 2011;352(2):329–340. doi:10.1016/j.ydbio.2011.01.038 [PubMed: 21300049]
74. Dickinson RJ, Keyse SM. Diverse physiological functions for dual-specificity MAP kinase phosphatases. *J Cell Sci.* 2006;119(22):4607–4615. doi:10.1242/jcs.03266 [PubMed: 17093265]
75. Li C, Scott DA, Hatch E, Tian X, Mansour SL. Dusp6 (Mkp3) is a negative feedback regulator of FGF-stimulated ERK signaling during mouse development. *Development.* 2007;134(1):167–176. doi:10.1242/dev.02701 [PubMed: 17164422]

76. Urness LD, Li C, Wang X, Mansour SL. Expression of ERK signaling inhibitors *Dusp6*, *Dusp7*, and *Dusp9* during mouse ear development. *Dev Dyn*. 2008;237(1):163–169. doi:10.1002/dvdy.21380 [PubMed: 18058922]
77. Mutai H, Nagashima R, Sugitani Y, Noda T, Fujii M, Matsunaga T. Expression of *Pou3f3/Brn-1* and its genomic methylation in developing auditory epithelium. *Dev Neurobiol*. 2009;69(14):913–930. doi:10.1002/dneu.20746 [PubMed: 19743445]
78. Diez-Roux G, Banfi S, Sultan M, et al. A High-Resolution Anatomical Atlas of the Transcriptome in the Mouse Embryo. *PLOS Biol*. 2011;9(1):e1000582. doi:10.1371/journal.pbio.1000582 [PubMed: 21267068]
79. Kumar S, Rathkolb B, Kemter E, et al. Generation and Standardized, Systemic Phenotypic Analysis of *Pou3f3L423P* Mutant Mice. *PLOS ONE*. 2016;11(3):e0150472. doi:10.1371/journal.pone.0150472 [PubMed: 27003440]
80. Goff LA, Groff AF, Sauvageau M, et al. Spatiotemporal expression and transcriptional perturbations by long noncoding RNAs in the mouse brain. *Proc Natl Acad Sci U S A*. 2015;112(22):6855–6862. doi:10.1073/pnas.1411263112 [PubMed: 26034286]
81. Oishi K, Aramaki M, Nakajima K. Mutually repressive interaction between *Brn1/2* and *Rorb* contributes to the establishment of neocortical layer 2/3 and layer 4. *Proc Natl Acad Sci U S A*. 2016;113(12):3371–3376. doi:10.1073/pnas.1515949113 [PubMed: 26951672]
82. Waldhaus J, Durruthy-Durruthy R, Heller S. Quantitative High-Resolution Cellular Map of the Organ of Corti. *Cell Rep*. 2015;11(9):1385–1399. doi:10.1016/j.celrep.2015.04.062 [PubMed: 26027927]
83. Usami S, Takumi Y, Suzuki N, et al. The localization of proteins encoded by *CRYM*, *KIAA1199*, *UBA52*, *COL9A3*, and *COL9A1*, genes highly expressed in the cochlea. *Neuroscience*. 2008;154(1):22–28. doi:10.1016/j.neuroscience.2008.03.018 [PubMed: 18448257]
84. Hawley SP, Wills MKB, Rabalski AJ, Bendall AJ, Jones N. Expression patterns of *ShcD* and *Shc* family adaptor proteins during mouse embryonic development. *Dev Dyn*. 2011;240(1):221–231. doi:10.1002/dvdy.22506 [PubMed: 21117147]
85. Wu L, Sagong B, Choi JY, Kim U-K, Bok J. A systematic survey of carbonic anhydrase mRNA expression during mammalian inner ear development. *Dev Dyn*. 2013;242(3):269–280. doi:10.1002/dvdy.23917 [PubMed: 23233153]
86. Radde-Gallwitz K, Pan L, Gan L, Lin X, Segil N, Chen P. Expression of *Islet1* marks the sensory and neuronal lineages in the mammalian inner ear. *J Comp Neurol*. 2004;477(4):412–421. doi:10.1002/cne.20257 [PubMed: 15329890]
87. Ficker M, Powles N, Warr N, Pirvola U, Maconochie M. Analysis of genes from inner ear developmental-stage cDNA subtraction reveals molecular regionalization of the otic capsule. *Dev Biol*. 2004;268(1):7–23. doi:10.1016/j.ydbio.2003.11.023 [PubMed: 15031101]
88. Chow C, Trivedi P, Pyle M, Matulle J, Fettiplace R, Gubbels SP. Evaluation of *Nestin* Expression in the Developing and Adult Mouse Inner Ear. *Stem Cells Dev*. 2016;25(19):1419–1432. doi:10.1089/scd.2016.0176 [PubMed: 27474107]
89. Chow CL, Guo W, Trivedi P, Zhao X, Gubbels SP. Characterization of a unique cell population marked by transgene expression in the adult cochlea of *nestin-CreER(T2)/tdTomato*-reporter mice. *J Comp Neurol*. 2015;523(10):1474–1487. doi:10.1002/cne.23747 [PubMed: 25611038]
90. Haugas M, Lillväli K, Hakanen J, Salminen M. *Gata2* is required for the development of inner ear semicircular ducts and the surrounding perilymphatic space. *Dev Dyn*. 2010;239(9):2452–2469. doi:10.1002/dvdy.22373 [PubMed: 20652952]
91. Koo SK, Hill JK, Hwang CH, Lin ZS, Millen KJ, Wu DK. *Lmx1a* maintains proper neurogenic, sensory, and non-sensory domains in the mammalian inner ear. *Dev Biol*. 2009;333(1):14–25. doi:10.1016/j.ydbio.2009.06.016 [PubMed: 19540218]
92. Mann ZF, Gálvez H, Pedreno D, et al. Shaping of inner ear sensory organs through antagonistic interactions between Notch signalling and *Lmx1a*. *eLife*. 2017;6:e33323. doi:10.7554/eLife.33323 [PubMed: 29199954]
93. Nichols DH, Pauley S, Jahan I, Beisel KW, Millen KJ, Fritzsche B. *Lmx1a* is required for segregation of sensory epithelia and normal ear histogenesis and morphogenesis. *Cell Tissue Res*. 2008;334(3):339–358. doi:10.1007/s00441-008-0709-2 [PubMed: 18985389]

94. Sánchez-Guardado LÓ, Ferran JL, Rodríguez-Gallardo L, Puelles L, Hidalgo-Sánchez M. Meis gene expression patterns in the developing chicken inner ear. *J Comp Neurol*. 2011;519(1):125–147. doi:10.1002/cne.22508 [PubMed: 21120931]
95. Morsli H, Choo D, Ryan A, Johnson R, Wu DK. Development of the mouse inner ear and origin of its sensory organs. *J Neurosci*. 1998;18(9):3327–3335. doi:10.1523/JNEUROSCI.18-09-03327.1998 [PubMed: 9547240]
96. Wang W, Chan EK, Baron S, Van De Water TR, Lufkin T. Hmx2 homeobox gene control of murine vestibular morphogenesis. *Development*. 2001;128(24):5017–5029. [PubMed: 11748138]
97. Poladia DP, Kish K, Kutay B, et al. Role of fibroblast growth factor receptors 1 and 2 in the metanephric mesenchyme. *Dev Biol*. 2006;291(2):325–339. doi:10.1016/j.ydbio.2005.12.034 [PubMed: 16442091]
98. Muzumdar MD, Tasic B, Miyamichi K, Li L, Luo L. A global double-fluorescent Cre reporter mouse. *Genesis*. 2007;45(9):593–605. doi:10.1002/dvg.20335 [PubMed: 17868096]
99. Dobin A, Davis CA, Schlesinger F, et al. STAR: ultrafast universal RNA-seq aligner. *Bioinformatics*. 2013;29(1):15–21. doi:10.1093/bioinformatics/bts635 [PubMed: 23104886]
100. Howe KL, Contreras-Moreira B, De Silva N, et al. Ensembl Genomes 2020-enabling non-vertebrate genomic research. *Nucleic Acids Res*. 2020;48(D1):D689–D695. doi:10.1093/nar/gkz890 [PubMed: 31598706]
101. Morgan M, Pagès H, Obenchain V, Hayden N. Rsamtools: Binary alignment (BAM), FASTA, variant call (BCF), and tabix file import. Published online 2018 R package version 1.32.0. <http://bioconductor.org/packages/Rsamtools>. doi:10.18129/B9.bioc.Rsamtools
102. Lawrence M, Huber W, Pagès H, et al. Software for Computing and Annotating Genomic Ranges. *PLOS Comput Biol*. 2013;9(8):e1003118. doi:10.1371/journal.pcbi.1003118 [PubMed: 23950696]
103. Risso D, Ngai J, Speed TP, Dudoit S. Normalization of RNA-seq data using factor analysis of control genes or samples. *Nat Biotechnol*. 2014;32(9):896. doi:10.1038/nbt.2931 [PubMed: 25150836]
104. Alexa A, Rahnenfuhrer J. topGO: Enrichment Analysis for Gene Ontology. Published online 2016 R package version 2.32.0. <https://bioconductor.org/packages/topGO>. doi:10.18129/B9.bioc.topGO
105. Huang M, Sage C, Li H, Xiang M, Heller S, Chen Z-Y. Diverse expression patterns of LIM-homeodomain transcription factors (LIM-HDs) in mammalian inner ear development. *Dev Dyn*. 2008;237(11):3305–3312. doi:10.1002/dvdy.21735 [PubMed: 18942141]
106. Winnier G, Blessing M, Labosky PA, Hogan BL. Bone morphogenetic protein-4 is required for mesoderm formation and patterning in the mouse. *Genes Dev*. 1995;9(17):2105–2116. doi:10.1101/gad.9.17.2105 [PubMed: 7657163]
107. Schindelin J, Arganda-Carreras I, Frise E, et al. Fiji: an open-source platform for biological-image analysis. *Nat Methods*. 2012;9(7):676–682. doi:10.1038/nmeth.2019 [PubMed: 22743772]
108. Avinash GB, Nuttall AL, Raphael Y. 3-D analysis of F-actin in stereocilia of cochlear hair cells after loud noise exposure. *Hear Res*. 1993;67(1):139–146. doi:10.1016/0378-5955(93)90241-R [PubMed: 8340265]
109. Mueller KL, Jacques BE, Kelley MW. Fibroblast Growth Factor Signaling Regulates Pillar Cell Development in the Organ of Corti. *J Neurosci*. 2002;22(21):9368–9377. doi:10.1523/JNEUROSCI.22-21-09368.2002 [PubMed: 12417662]
110. Edgar R, Domrachev M, Lash AE. Gene Expression Omnibus: NCBI gene expression and hybridization array data repository. *Nucleic Acids Res*. 2002;30(1):207–210. doi:10.1093/nar/30.1.207 [PubMed: 11752295]

Key findings:

- Translating Ribosome Affinity Purification (TRAP) targeting the Fgf20-Cre lineage enriched for organ of Corti progenitor RNA
- TRAP combined with RNAseq (TRAPseq) identified genes downstream of FGF20 during organ of Corti differentiation
- FGF20 regulates *Sall1*, gene implicated in human sensorineural hearing loss
- *Sall1* mutant mice exhibit a decrease in the number of organ of Corti outer hair cells

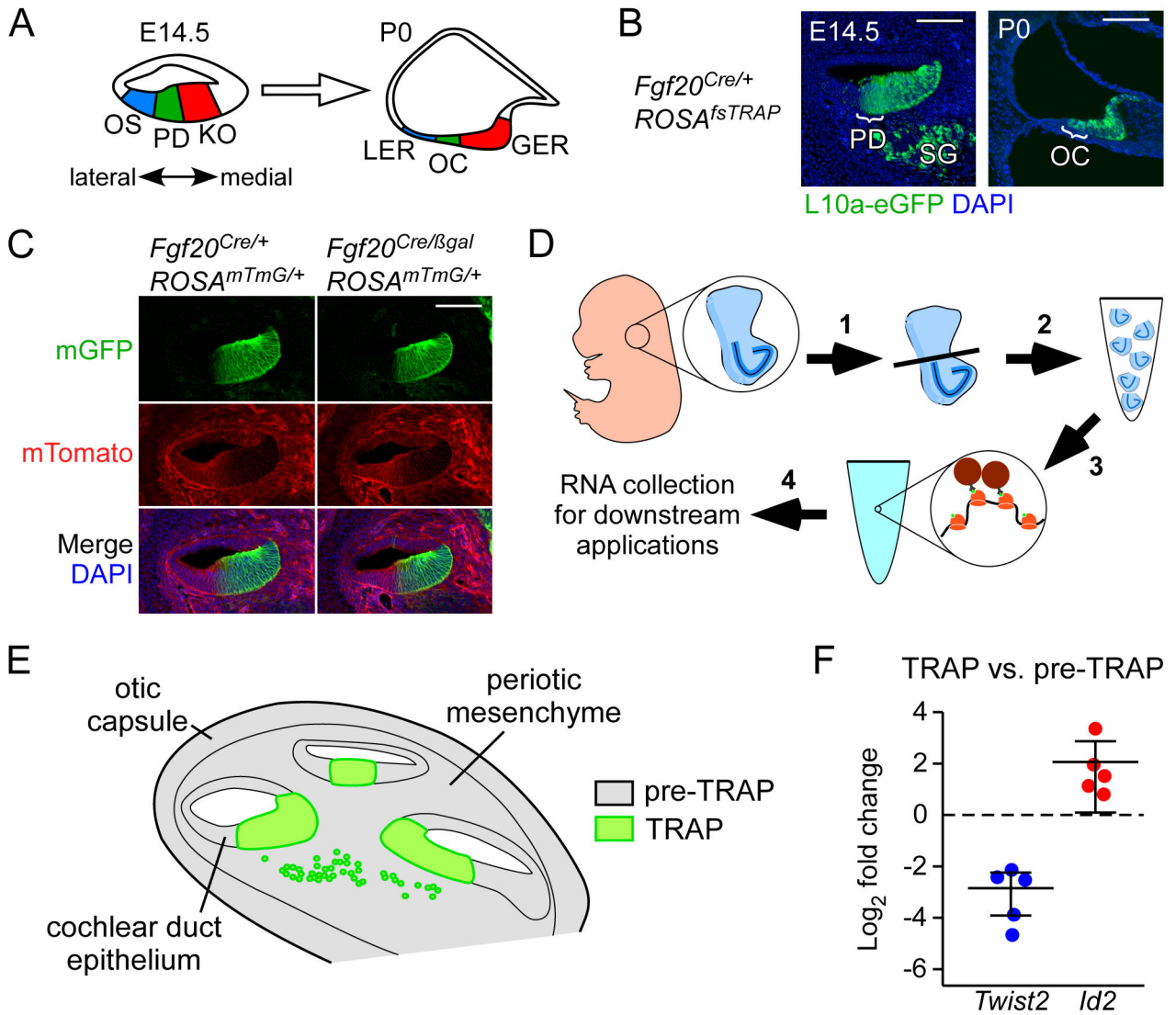


Figure 1. *Fgf20^{Cre}* targets L10a-eGFP expression to the prosensory domain and Kölliker's organ (A) Schematic representing cross-sectional view through the E14.5 and P0 cochlear duct. At E14.5, the epithelium at the cochlear duct floor can be divided into three regions: outer sulcus (OS), prosensory domain (PD), and Kölliker's organ (KO). Cells from these three regions contribute to the lesser epithelial ridge (LER), organ of Corti (OC), and greater epithelial ridge (GER), respectively, at P0. Double-headed arrow indicates medial (neural) and lateral (abneural) directions. In all figures, sections through the cochlear duct are presented in this orientation.

(B) Sections through the middle turn of E14.5 and P0 *Fgf20^{Cre/+}; ROSA^{fsTRAP/+}* cochlear ducts, showing L10a-eGFP (green) expression. At E14.5, L10a-eGFP is found in the prosensory domain (PD; bracket), Kölliker's organ and medial wall, and spiral ganglion (SG). At P0, it is found in the organ of Corti (OC; bracket), greater epithelial ridge, and medial wall. DAPI, nuclei (blue); scale bar, 100 μ m.

(C) Section through the middle turn of E14.5 cochlear ducts from *Fgf20^{Cre/+}; ROSA^{mTmG/+}* and *Fgf20^{Cre/βgal}; ROSA^{mTmG/+}* embryos. Cells of the *Fgf20^{Cre}* lineage express mGFP (mG),

green); non-lineage cells express mTomato (mT, red). DAPI, nuclei (blue); scale bar, 100 μm .

(D) Schematic showing an overview of the TRAPseq protocol (see Experimental Procedures). 1) Ventral otocysts containing the cochlea were dissected from E14.5 embryos. 2) Otocysts from each litter were pooled according to genotype to increase RNA yield. 3) Otocysts were then homogenized and centrifuged to make polysomes (pre-TRAP samples were collected at this stage). This was followed by immunoprecipitation with anti-GFP antibodies to collect L10a-eGFP labelled polysomes. 4) This produced TRAP samples, which were then purified for RNA along with pre-TRAP samples and used for downstream applications.

(E) Schematic of a cross-sectional view of the E14.5 ventral otocyst, showing three turns of the cochlear duct, surrounded by periotic mesenchyme and otic capsule. Pre-TRAP RNA (representing total input tissue) comes from the cochlear duct epithelium, periotic mesenchyme, and otic capsule (gray). TRAP RNA (representing *Fgf20^{Cre}*-lineage tissue, which expresses L10a-eGFP) comes from the prosensory domain, Kölliker's organ, medial wall of the cochlear duct, and some cells of the spiral ganglion (green).

(F) qRT-PCR showing fold change in *Twist2* and *Id2* expression (normalized to *Gadph*) in TRAP RNA samples compared to pre-TRAP samples from *Fgf20^{Cre/+}; ROSA^{mTmG/+}* E14.5 cochleae. Each dot represents an RNA sample pooled from at least 3 embryos.

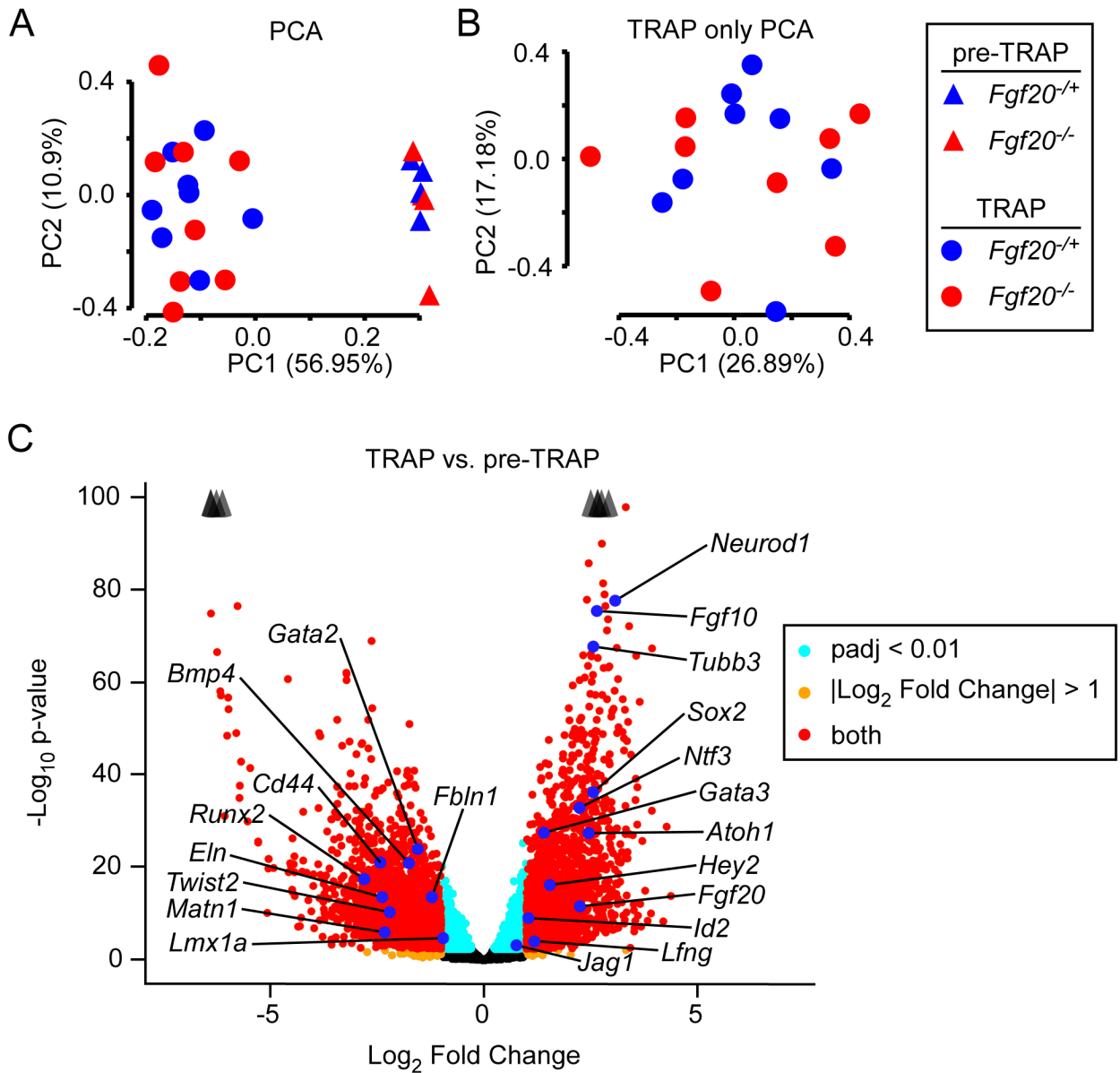


Figure 2. *Fgf20^{Cre}* TRAPseq enriched for prosensory domain RNA
 (A) Principal Component Analysis (PCA) on 24 TRAPseq samples (8 pre-TRAP samples – 4 *Fgf20^{+/-}*, 4 *Fgf20^{-/-}*; 16 TRAP samples – 8 *Fgf20^{+/-}*, 8 *Fgf20^{-/-}*) showing separation of pre-TRAP and TRAP samples along PC1, but not of *Fgf20^{+/-}* and *Fgf20^{-/-}* samples.
 (B) PCA on the 16 TRAP samples (excluding the 8 pre-TRAP samples) also did not show separation between *Fgf20^{+/-}* and *Fgf20^{-/-}* samples along the first two principal components.
 (C) Volcano plot showing TRAP vs. pre-TRAP differentially expressed genes. Positive Log_2 Fold Change value indicates enrichment by TRAP; negative Log_2 Fold Change value indicates depletion by TRAP. Labeled genes represent markers of the prosensory domain, Kölliker’s organ, spiral ganglion, outer sulcus, periotic mesenchyme, and otic capsule. Padj, adjusted p-value for multiple comparisons (Benjamini-Hochberg method). The p-value plotted on y-axis is unadjusted. Arrowheads indicate genes above y-axis range.

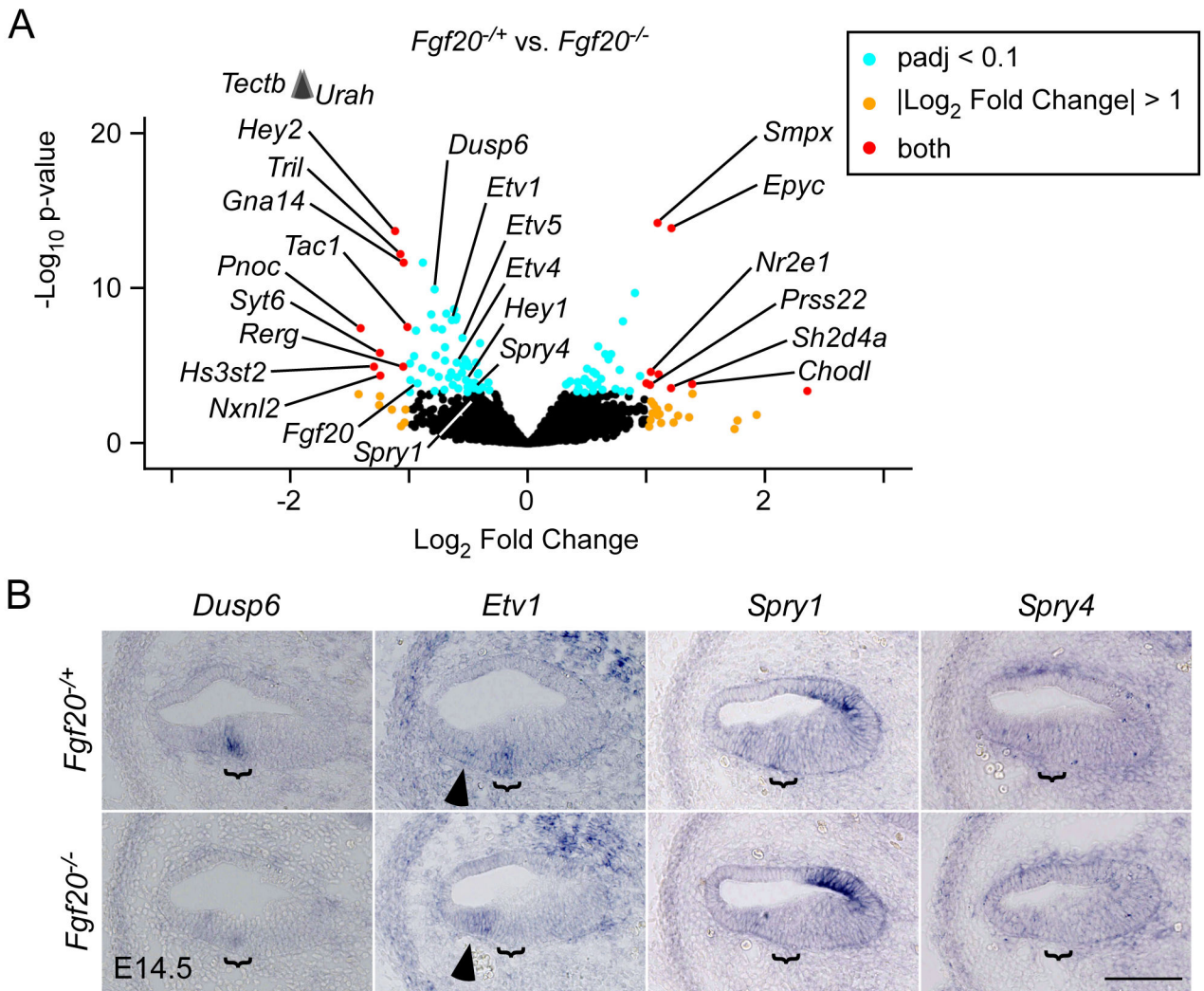


Figure 3. TRAPseq revealed known FGF target genes during organ of Corti differentiation downstream of *Fgf20*

(A) Volcano plot showing *Fgf20^{+/+}* vs. *Fgf20^{-/-}* differentially expressed genes. *Fgf20*, transcripts associated with FGF signaling, and transcripts meeting the criteria padj < 0.1 and Log₂ Fold Change < -1 or > 1 are labeled, with the exception of predicted genes and unnamed transcripts. padj, adjusted p-value for multiple comparisons (Benjamini-Hochberg method). The p-value plotted on the y-axis is unadjusted. Arrowheads indicate genes above the y-axis range.

(B) RNA in situ hybridization for known FGF target genes *Dusp6*, *Etv1*, *Spry1*, and *Spry4* on sections through the middle turn of E14.5 *Fgf20^{+/+}* (*Fgf20^{Cre/+}*) and *Fgf20^{-/-}* (*Fgf20^{Cre/βgal}*) cochlear ducts. Bracket, prosensory domain. Arrowhead, increased expression of *Etv1* in the outer sulcus of *Fgf20^{-/-}* cochleae. Scale bar, 100 μm.

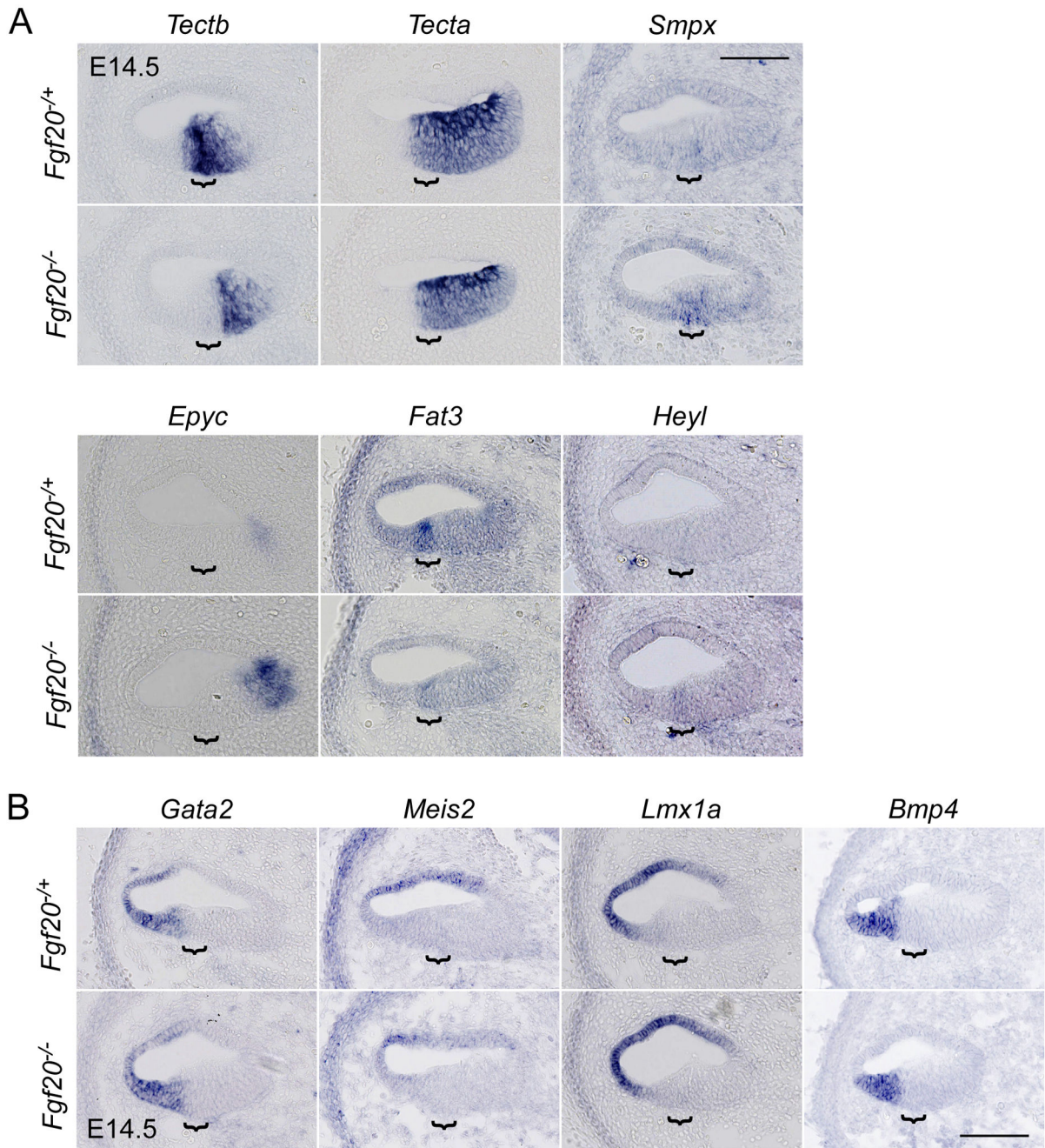


Figure 4. Expression analysis of genes identified by TRAPseq associated with cochlea development or hearing loss downstream of *Fgf20*
 RNA in situ hybridization on sections through the middle turn of E14.5 *Fgf20*^{+/+} (*Fgf20*^{Cre/+}) and *Fgf20*^{-/-} (*Fgf20*^{Cre/βgal}) cochlear ducts. Bracket, prosensory domain. Scale bar, 100 μm.
 (A) Genes expressed within the *Fgf20*^{Cre} lineage: *Tectb*, *Tecta*, *Smpx*, *Epyc*, *Fat3*, and *Heyl*
 (B) Genes expressed outside of the *Fgf20*^{Cre} lineage: *Gata2*, *Meis2*, *Lmx1a*, and *Bmp4*

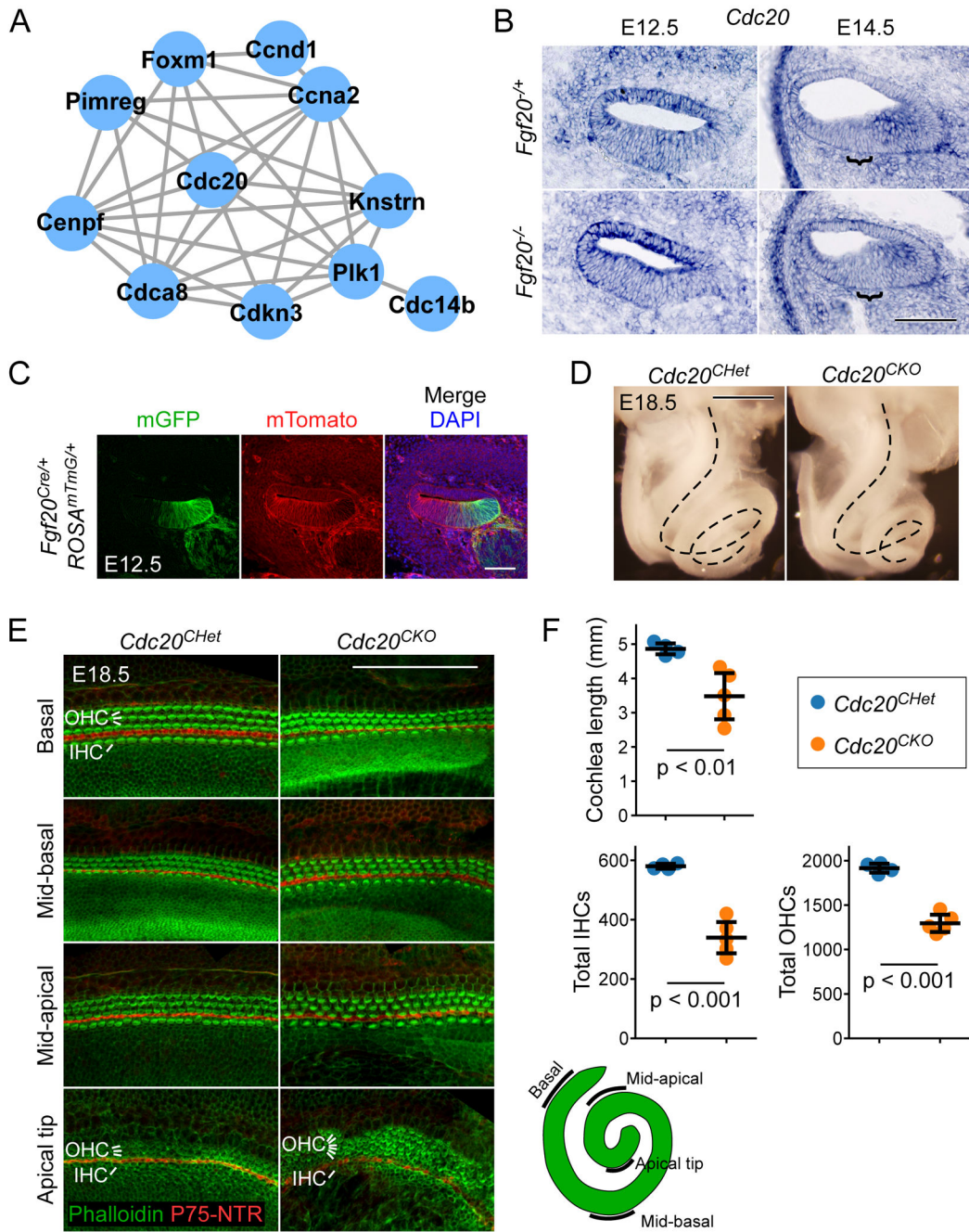


Figure 5. Conditional deletion of *Cdc20* with *Fgf20^{Cre}* resulted in a shorter cochlea
 (A) The largest protein-protein interaction network identified via the STRING database consisted of genes involved in cell cycle regulation. Lines represent known and predicted protein-protein interactions of high or very high confidence (minimum required interaction score = 0.700).
 (B) RNA in situ hybridization for *Cdc20* on sections through the middle turn of E12.5 and E14.5 *Fgf20^{-/+}* (*Fgf20^{Cre/+}*) and *Fgf20^{-/-}* (*Fgf20^{Cre/βgal}*) cochlear ducts. Bracket, prosensory domain. Scale bar, 100 μm.
 (C) mGFP and mTomato expression in *Fgf20^{Cre/+}* *ROSA^{tmTomG/+}* at E12.5.
 (D) *Cdc20^{CHet}* and *Cdc20^{CKO}* embryos at E18.5.
 (E) Histological sections of the cochlea at E18.5 for *Cdc20^{CHet}* and *Cdc20^{CKO}* genotypes, stained for Phalloidin and P75-NTR.
 (F) Quantitative analysis of cochlea length, total IHCs, and total OHCs.

(C) Section through the middle turn of E12.5 *Fgf20^{Cre/+};ROSA^{mTmG/+}* cochlear duct. Cells of the *Fgf20^{Cre}* lineage express mGFP (mG, green); non-lineage cells express mTomato (mT, red). DAPI, nuclei (blue); scale bar, 100 μ m.

(D) Dissected inner ears from E18.5 *Cdc20^{CHet} (Fgf20^{Cre/+};Cdc20^{flox/+})* and *Cdc20^{CKO} (Fgf20^{Cre/+};Cdc20^{flox/flox})* embryos with the otic capsule removed to reveal the coiled cochlea (dotted lines). Scale bar, 0.5 mm.

(E) Whole mount cochlea from E18.5 *Cdc20^{CHet}* and *Cdc20^{CKO}* embryos showing one row of inner hair cells (IHC) and three rows of outer hair cells (OHC) marked by phalloidin (green) and separated by inner pillar cells (p75NTR, red). Representative regions from the basal, mid-basal, and mid-apical turns, and apical tip of the cochlea are shown. See schematic showing locations of the turns of the cochlea. At the apical tip, four or more rows of OHCs were frequently observed in *Cdc20^{CHet}* cochleae. Scale bar, 100 μ m.

(F) Quantification of cochlea length and total number of inner and outer hair cells (IHCs and OHCs) in E18.5 *Cdc20^{CHet}* (n = 4) and *Cdc20^{CKO}* (n = 5) cochleae. Error bars represent mean \pm std. Results were analyzed by Student's t-test; p-values are shown.

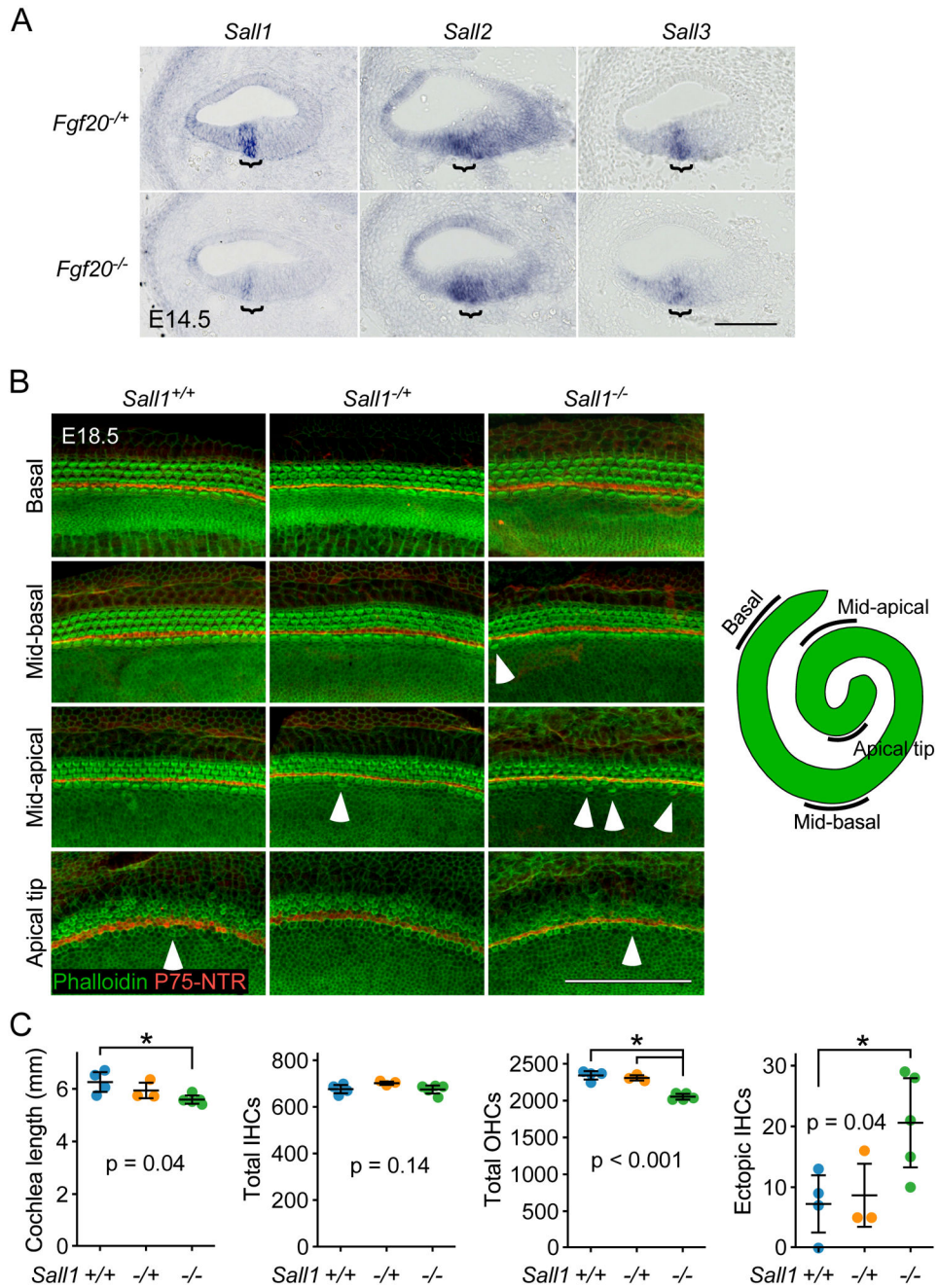


Figure 6. *Sall1*^{-/-} cochleae exhibit an outer hair cell phenotype

(A) RNA in situ hybridization for *Sall1*, *Sall2*, and *Sall3* on sections through the middle turn of E14.5 *Fgf20*^{-/+} (*Fgf20*^{Cre/+}) and *Fgf20*^{-/-} (*Fgf20*^{Cre/βgal}) cochlear ducts. Bracket, prosensory domain. Scale bar, 100 μm.

(B) Whole mount cochlea from E18.5 *Sall1*^{+/+}, *Sall1*^{-/-}, and *Sall1*^{-/-} embryos showing inner hair cells and outer hair cells marked by phalloidin (green) and separated by inner pillar cells (p75NTR, red). Representative regions from the basal (5% of total length from the basal tip), mid-basal (33%), and mid-apical (67%) turns, and apical tip (90%) of the cochlea are shown. See schematic showing locations of the turns of the cochlea. Numerous

ectopic inner hair cells were found throughout *Sall1*^{-/-} cochleae, especially towards the apex (arrowheads). Scale bar, 100 μ m.

(C) Quantification of cochlea length, total number of inner hair cells (IHCs) and outer hair cells (OHCs), and total number of ectopic IHCs in E18.5 *Sall1*^{+/+} (n = 4), *Sall1*^{-/+} (n = 3), and *Sall1*^{-/-} (n = 5) cochleae. Error bars represent mean \pm std. Results were analyzed by one-way ANOVA. P-values shown are from the ANOVA. * indicates $p < 0.05$ from Tukey's HSD (ANOVA post-hoc).

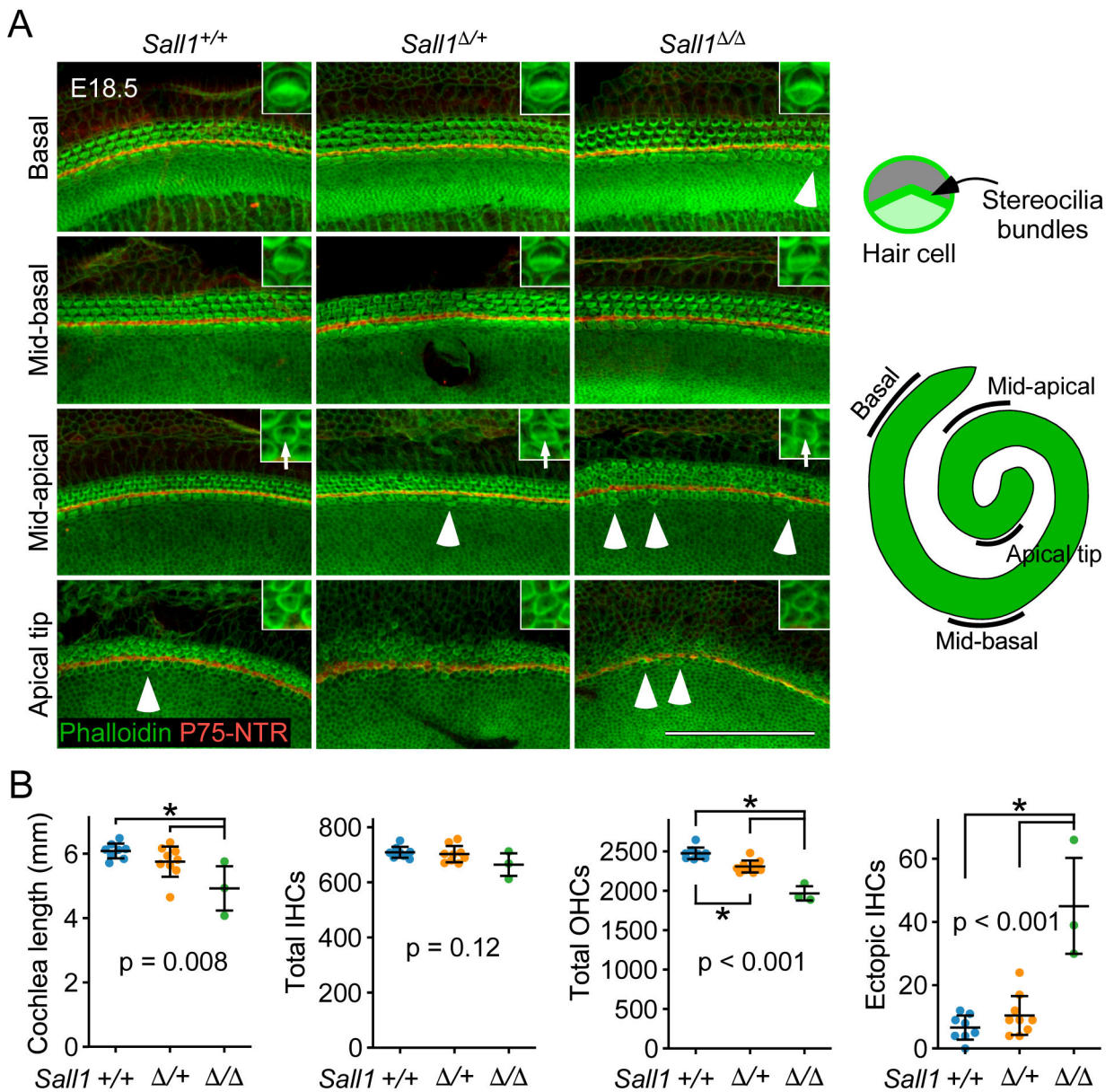


Figure 7. *Sall1- Zn2-10* mutant cochleae exhibit a more severe phenotype than *Sall1*^{-/-} cochleae

(A) Whole mount cochlea from E18.5 *Sall1*^{+/+}, *Sall1*^{Δ/+}, and *Sall1*^{Δ/Δ} embryos showing inner hair cells and outer hair cells marked by phalloidin (green) and separated by inner pillar cells (p75NTR, red). Representative regions from the basal (5% of total length from the basal tip), mid-basal (33%), and mid-apical (67%) turns, and apical tip (90%) of the cochlea are shown. See schematic to the right showing locations of the turns of the cochlea. Inset: 3.8x magnified image of a representative OHC showing stereocilia bundle formation (arrows in mid-apical region). Numerous ectopic inner hair cells were found throughout *Sall1*^{Δ/Δ} cochleae, especially towards the apex (arrowheads). Scale bar, 100 μm.

(B) Quantification of cochlea length, total number of inner hair cells (IHCs) and outer hair cells (OHCs), and total number of ectopic IHCs in E18.5 *Sall1*^{+/+} (n = 8), *Sall1*^{Δ/+} (n = 9), and *Sall1*^{Δ/Δ} (n = 3) cochleae. Error bars represent mean ± std. Results were analyzed by

one-way ANOVA. P-values shown are from the ANOVA. * indicates $p < 0.05$ from Tukey's HSD (ANOVA post-hoc).

Author Manuscript

Author Manuscript

Author Manuscript

Author Manuscript

Table 1.

Top 12 gene ontology (GO) terms from a list of 2017 differentially expressed genes depleted by TRAP, compared to pre-TRAP samples, in *Fgf20^{Cre/+}; ROSA^{fsTRAP/+}* cochleae.

Rank*	GO ID	GO biological processes term	p-value
1	GO:0006954	inflammatory response	3.30E-15
2	GO:0001525	angiogenesis	1.60E-12
3	GO:0030198	extracellular matrix organization	2.20E-11
4	GO:0045766	positive regulation of angiogenesis	2.20E-10
5	GO:0070374	positive regulation of ERK1 and ERK2 cascade	2.70E-10
6	GO:0001974	blood vessel remodeling	3.20E-10
7	GO:0007155	cell adhesion	8.80E-10
8	GO:0030593	neutrophil chemotaxis	2.00E-09
9	GO:0002548	monocyte chemotaxis	8.70E-09
10	GO:0007186	G-protein coupled receptor signaling pathway	5.10E-08
11	GO:0090090	negative regulation of canonical Wnt signaling pathway	2.20E-07
12	GO:0001958	endochondral ossification	2.80E-07

* Rank determined by p-value (lowest to highest).

Table 2.

Top 12 gene ontology (GO) terms from a list of 1833 differentially expressed genes enriched by TRAP, compared to pre-TRAP samples, in *Fgf20^{Cre/+};ROSA^{fsTRAP/+}* cochleae.

Rank*	GO ID	GO biological processes term	p-value
1	GO:0007605	sensory perception of sound	6.30E-09
2	GO:0007411	axon guidance	3.30E-08
3	GO:0048791	calcium ion-regulated exocytosis of neurotransmitter	7.00E-08
4	GO:0048172	regulation of short-term neuronal synaptic plasticity	1.20E-06
5	GO:0042391	regulation of membrane potential	2.00E-06
6	GO:0007626	locomotory behavior	3.00E-06
7	GO:0050885	neuromuscular process controlling balance	3.60E-06
8	GO:0019228	neuronal action potential	7.20E-06
9	GO:0014059	regulation of dopamine secretion	9.90E-06
10	GO:0017158	regulation of calcium ion-dependent exocytosis	1.10E-05
11	GO:0060088	auditory receptor cell stereocilium organization	1.70E-05
12	GO:0045665	negative regulation of neuron differentiation	2.30E-05

* Rank determined by p-value (lowest to highest).

Table 3.

Select top gene ontology (GO) terms from a list of top 362 *Fgf20*^{-/+} vs. *Fgf20*^{-/-} differentially expressed genes from TRAPseq.

Rank*	GO ID	GO biological processes term	p-value
1	GO:0003184	pulmonary valve morphogenesis	5.40E-06
2	GO:0045664	regulation of neuron differentiation	6.80E-05
3	GO:0007605	sensory perception of sound	1.50E-04
5	GO:0007601	visual perception	3.60E-04
6	GO:0001709	cell fate determination	4.10E-04
7	GO:0046426	negative regulation of JAK-STAT cascade	4.10E-04
9	GO:0021879	forebrain neuron differentiation	6.10E-04
12	GO:0051301	cell division	1.12E-03
13	GO:0021795	cerebral cortex cell migration	1.21E-03
14	GO:0009948	anterior/posterior axis specification	1.23E-03
21	GO:0090596	sensory organ morphogenesis	1.77E-03
28	GO:0043583	ear development	2.50E-03
30	GO:2000177	regulation of neural precursor cell proliferation	2.70E-03
33	GO:0045596	negative regulation of cell differentiation	3.29E-03
35	GO:0031175	neuron projection development	3.46E-03
38	GO:0060113	inner ear receptor cell differentiation	4.33E-03
39	GO:0007050	cell cycle arrest	4.76E-03

*Rank determined by p-value (lowest to highest).

Table 4.

Fgf20^{-/+} vs. *Fgf20*^{-/-} differentially expressed genes from TRAPseq associated with FGF signaling.

Rank [*]	Ensembl ID	Gene	Enrichment [^]	Log2FC ^{&}	padj [#]
9	ENSMUSG00000019960	<i>Dusp6</i>	enriched	-0.79	<0.001
21	ENSMUSG00000004151	<i>Etv1</i>	depleted	-0.72	<0.001
36	ENSMUSG00000017724	<i>Etv4</i>	ENRICHED	-0.60	<0.01
23	ENSMUSG00000013089	<i>Etv5</i>	-	-0.55	<0.001
74	ENSMUSG00000031603	<i>Fgf20</i>	ENRICHED	-0.93	0.03
50	ENSMUSG00000040289	<i>Hey1</i>	ENRICHED	-0.55	0.01
5	ENSMUSG00000019789	<i>Hey2</i>	ENRICHED	-1.12	<0.001
106	ENSMUSG00000037211	<i>Spry1</i>	ENRICHED	-0.45	0.10
87	ENSMUSG00000024427	<i>Spry4</i>	depleted	-0.45	0.06

* Rank determined by padj (lowest to highest).

[^] Enrichment by TRAP: results of TRAP vs. pre-TRAP comparison in *Fgf20*^{Cre/+}; *ROSA*^{fsTRAP/+} cochleae. Dash (-) indicates padj > 0.05; otherwise padj < 0.05. “enriched” indicates Log₂ Fold Change > 0; “ENRICHED” indicates Log₂ Fold Change > 1. “depleted” indicates Log₂ Fold Change < 0; “DEPLETED” indicates Log₂ Fold Change < -1.

[&] Log₂ Fold Change of *Fgf20*^{-/+} vs. *Fgf20*^{-/-} comparison.

[#] Adjusted p-value of *Fgf20*^{-/+} vs. *Fgf20*^{-/-} comparison.

Table 5.

Fgf20^{-/+} vs. *Fgf20*^{-/-} differentially expressed genes from TRAPseq associated with hearing or cochlear development.

Rank*	Ensembl ID	Gene	Enrichment [^]	Log2FC ^{&}	padj [#]
236	ENSMUSG00000021835	<i>Bmp4</i>	DEPLETED	0.41	0.38
10	ENSMUSG00000028222	<i>Calb1</i>	ENRICHED	0.90	<0.001
16	ENSMUSG00000027555	<i>Car13</i>	enriched	-0.64	<0.001
331	ENSMUSG0000003031	<i>Cdkn1b</i>	-	-0.43	0.47
11	ENSMUSG00000030862	<i>Cpxm2</i>	enriched	-0.62	<0.001
12	ENSMUSG00000030905	<i>Crym</i>	depleted	-0.69	<0.001
4	ENSMUSG00000019936	<i>Epyc</i>	depleted	1.21	<0.001
31	ENSMUSG00000074505	<i>Fat3</i>	-	-0.96	<0.01
47	ENSMUSG00000015053	<i>Gata2</i>	DEPLETED	0.55	<0.01
28	ENSMUSG00000032744	<i>Hey1</i>	DEPLETED	0.65	<0.01
119	ENSMUSG00000050100	<i>Hmx2</i>	-	0.74	0.11
96	ENSMUSG00000026686	<i>Lmx1a</i>	depleted	0.55	0.08
49	ENSMUSG00000098318	<i>Lockd</i>	-	-0.65	0.01
29	ENSMUSG00000036446	<i>Lum</i>	-	0.70	<0.01
61	ENSMUSG00000027210	<i>Meis2</i>	DEPLETED	0.48	0.02
168	ENSMUSG00000030739	<i>Myh14</i>	ENRICHED	-0.41	0.23
97	ENSMUSG00000004891	<i>Nes</i>	DEPLETED	-0.78	0.08
83	ENSMUSG00000060424	<i>Pantr1</i>	depleted	-0.51	0.05
53	ENSMUSG00000045515	<i>Pou3f3</i>	depleted	-0.42	0.01
71	ENSMUSG00000031665	<i>Sall1</i>	enriched	-0.49	0.03
177	ENSMUSG00000049532	<i>Sall2</i>	ENRICHED	-0.39	0.26
89	ENSMUSG00000024565	<i>Sall3</i>	enriched	-0.59	0.06
14	ENSMUSG00000035109	<i>Shc4</i>	ENRICHED	-0.60	<0.001
3	ENSMUSG00000041476	<i>Smpx</i>	ENRICHED	1.09	<0.001
225	ENSMUSG00000074637	<i>Sox2</i>	ENRICHED	-0.45	0.37
18	ENSMUSG00000061762	<i>Tac1</i>	-	-1.01	<0.001
161	ENSMUSG00000037705	<i>Tecta</i>	ENRICHED	-0.36	0.22
1	ENSMUSG00000024979	<i>Tectb</i>	ENRICHED	-1.91	<0.001
128	ENSMUSG00000021779	<i>Thrb</i>	ENRICHED	0.45	0.13

* Rank determined by padj (lowest to highest).

[^] Enrichment by TRAP: results of TRAP vs. pre-TRAP comparison in *Fgf20*^{Cre/+}; *ROSA*^{fsTRAP/+} cochleae. Dash (-) indicates padj > 0.05; otherwise padj < 0.05. “enriched” indicates Log₂ Fold Change > 0; “ENRICHED” indicates Log₂ Fold Change > 1. “depleted” indicates Log₂ Fold Change < 0; “DEPLETED” indicates Log₂ Fold Change < -1.

[&] Log₂ Fold Change of *Fgf20*^{-/+} vs. *Fgf20*^{-/-} comparison.

[#] Adjusted p-value of *Fgf20*^{-/+} vs. *Fgf20*^{-/-} comparison.

Table 6.

Fgf20^{-/+} vs. *Fgf20*^{-/-} differentially expressed genes from TRAPseq associated with cell cycle regulation.

Rank [*]	Ensembl ID	Gene	Enrichment [^]	Log2FC ^{&}	padj [#]
70	ENSMUSG00000027715	<i>Ccna2</i>	depleted	-0.33	0.03
32	ENSMUSG00000070348	<i>Ccnd1</i>	-	-0.53	<0.01
120	ENSMUSG00000033102	<i>Cdc14b</i>	-	-0.49	0.11
24	ENSMUSG00000006398	<i>Cdc20</i>	depleted	-0.40	<0.001
222	ENSMUSG00000024791	<i>Cdca5</i>	-	-0.30	0.37
183	ENSMUSG00000028873	<i>Cdca8</i>	-	-0.33	0.28
197	ENSMUSG00000019942	<i>Cdk1</i>	depleted	-0.29	0.31
206	ENSMUSG00000026023	<i>Cdk15</i>	ENRICHED	-0.45	0.32
121	ENSMUSG00000037628	<i>Cdkn3</i>	depleted	-0.41	0.12
159	ENSMUSG00000026605	<i>Cenpf</i>	-	-0.92	0.22
158	ENSMUSG0000001517	<i>Foxm1</i>	depleted	-0.43	0.22
95	ENSMUSG00000027331	<i>Knstrn</i>	-	-0.32	0.07
146	ENSMUSG00000020808	<i>Pimreg</i>	-	-0.37	0.18
147	ENSMUSG00000030867	<i>Plk1</i>	depleted	-0.38	0.18

* Rank determined by padj (lowest to highest).

[^] Enrichment by TRAP: results of TRAP vs. pre-TRAP comparison in *Fgf20*^{Cre/+}; *ROSA*^{lsTRAP/+} cochleae. Dash (-) indicates padj > 0.05; otherwise padj < 0.05. "enriched" indicates Log₂ Fold Change > 0; "ENRICHED" indicates Log₂ Fold Change > 1. "depleted" indicates Log₂ Fold Change < 0; "DEPLETED" indicates Log₂ Fold Change < -1.

[&] Log₂ Fold Change of *Fgf20*^{-/+} vs. *Fgf20*^{-/-} comparison.

[#] Adjusted p-value of *Fgf20*^{-/+} vs. *Fgf20*^{-/-} comparison.